ESA Climate Change Initiative (CCI)

Sea Level Budget Closure (SLBC_cci)

Sea Level Budget Closure Assessment Report
ESA_SLBC_cci_D3.2

(Version 1.1, issued 08 March 2019)

SLBC Assessment Report 2 based on version 1 data

Prime & Science Lead:	Martin Horwath Technische Universität Dresden (TUDr) Martin.Horwath@tu-dresden.de
Technical Officer:	Jérôme Benveniste ESA ESRIN, Frascati, Italy Jerome.Benveniste@esa.int
Consortium:	Technische Universität Dresden (TUDr) Laboratoire d'Etudes en Géophysique et Océanographie Spatiales (LEGOS) Universität Bremen (UB) Universität Zürich (UZH) University of Leeds (UoL) Goethe-Universität Frankfurt (GUF) Danmarks Tekniske Universitet, DTU Space, Geodynamics (DTU-GDK) Danmarks Tekniske Universitet, DTU Space, Geodesy (DTU-GEK) Nansen Environmental and Remote Sensing Center (NERSC) University of Reading (UoR) Mercator Ocean, Toulouse (MerO)

To be cited as:

Horwath, M.; Novotny, K.; Cazenave, A.; Palanisamy, H.; Marzeion, B.; J.-H. Malles; Paul, F.; Döll, P.; Cáceres, D.; Hogg, A.; Shepherd, A.; Otosaka, I.; Forsberg, R.; Barletta, V.R.; Andersen, O.B.; Ranndal, H.; Johannessen, J.; Nilsen, J.E.; Gutknecht, B.D.; Merchant, Ch.J.; von Schuckmann, K.: *ESA Climate Change Initiative (CCI) Sea Level Budget Closure (SLBC_cci). Product Description Document D3.2: SLBC Assessment Report 2 based on version 1 data. Version 1.1, 08 March 2019.*

Signatures page

Prepared by	Kristin Novotny Project Manager, TUDr Martin Horwath Science Leader, TUDr Anny Cazenave, Hindumathi Palanisamy, LEGOS; Ben Marzeion, UB; Frank Paul, Raymond Le Bris, UZH; Petra Döll, Denise Cáceres, GUF; Anna Hogg, Andrew Shepherd, UOL; Rene Forsberg, DTU-GDK; Ole B. Andersen, Heidi Ranndal, DTU-GEK; Johnny Johannessen, Jan Even O. Nilsen, NERSC; Benjamin D. Gutknecht, TUDr; Christopher John Merchant, Claire Rachel MacIntosh, UoR; Karina von Schuckmann, MerO	Date: 2019-03-08
Checked by	Martin Horwath Science Leader, TUDr	Date: 2019-03-08
Approved by	Jérôme Benveniste Technical Officer, ESA	Date:

Change Log

Issue	Author, Org.	Affected Section	Reason/Description	Status
1.0	M. Horwath / TUDr	All	Document Creation	Released to ESA 2018-12-20
1.1	M.Horwath / TUDr	All	Document revision after review by ESA	Released to ESA 2019-03-08

Distribution List

Organization	Consortium Member
TUDr	Martin Horwath
LEGOS	Anny Cazenave
UB	Ben Marzeion
UZH	Frank Paul
UoL	Andrew Shepherd, Anna Hogg
DTU- GDK	Rene Forsberg
GUF	Petra Döll
NERSC	Johnny Johannessen
DTU-GEK	Ole B. Andersen
UoR	Christopher Merchant
MerO	Karina von Schuckmann
ESA	Jérôme Benveniste Marco Restano Américo Ambrózio

Table of Contents

Acronyms and Abbreviations

Acronym	Explanation
AIS	Antarctic Ice Sheet
Argo	global array of temperature/salinity profiling floats
ARMOR3D	A 3D multi-observations T,S,U,V product of the ocean
CCI, cci	Climate Change Initiative (initiated by ESA)
C-GLORS	CMCC Global Ocean Reanalysis System
CMC	Continental Mass Change
CMCC	Centro Euro-Mediterraneo sui Cambiamenti Climatici (Euro-Mediterranean Center on Climate Change)
CMEMS	Copernicus Marine Environment Monitoring Service
CRU	Climatic Research Unit (University of East Anglia, Norwich, UK)
CRU TS	CRU Timeseries (grids of observed climate)
CSR	Center for Space Research (University of Texas at Austin)
CTD	conductivity, temperature, and depth
DTU	Danmarks Tekniske Universitet
DTU-GDK	DTU, Geodynamics Group
e.s.l.	equivalent sea level
EN4	version 4 of the Met Office Hadley Centre ‘‘EN’’ series of data sets of global quality controlled ocean temperature and salinity profiles
Envisat	"Environmental Satellite", Earth-observing satellite operated by ESA
ERS-1/2	European Remote Sensing Satellite -1/2
ESA	European Space Agency
GAA, GAB, GAC, GAD	Names of data products related to GRACE atmospheric and oceanic background models (refer to section 3.2.2)
GFO	GRACE Follow-On mission
GFZ	GeoForschungsZentrum Potsdam
GIA	Glacial Isostatic Adjustment
GIS	Greenland Ice Sheet
GLORYS	Gobal Ocean Reanalyis and Simulation (at Mercator Ocean)
GMB	Gravimetric Mass Balance / GRACE Mass Balance
GMSL	Global Mean Sea Level
GPCC	Global Precipitation Climatology Centre
GRACE	Gravity Recovery and Climate Experiment
GRDC	Global Run-off Data Center
GSFC	Goddard Space Flight Center
GT, Gt	Gigatons
IBE	Inverse Barometer Effect
ICE-5G	models of postglacial relative sea-level history
ICESat	Ice, Cloud, and land Elevation Satellite, part of NASA's Earth Observing System
IMBIE	Ice Sheet Mass Balance Inter-comparison Exercise

IOM	Input-Output-Method
IPRC	International Pacific Research Center
ITSG	Institute of Geodesy, Theoretical Geodesy and Satellite Geodesy (TU Graz)
JAMSTEC	Japan Agency for Marine-earth Science and Technology
JPL	Jet Propulsion Laboratory
LEGOS	Laboratoire d'Etudes en Géophysique et Océanographie Spatiales
LWS	Land Water Storage
NERSC	Nansen Environmental and Remote Sensing Center
NOAA	National Oceanic and Atmospheric Administration
OMC	Ocean Mass Change
ORAS4, ORAS5	Ocean Reanalysis System 4
RL05, RL06	(GRACE) solution Release 05/06
RMS	Root Mean Square
RSS	Root Square Sum
SARAL	Satellite with ARgos and ALtiKa, cooperative altimetry technology mission of Indian Space Research Organisation (ISRO) and CNES (Space Agency of France)
SCRIPPS	Scripps Institution of Oceanography (University of California)
SH	spherical harmonic
SL_cci	ESA CCI_Sea Level Project
SLBC	Sea Level Budget Closure
SLE	Sea Level Equivalent
SOC	Sum Of Components
SSLA	Steric Sea Level Anomaly
STD	Standard Deviation
T&S	Temperature and Salinity
TOPAZ	(Towards) an Operational Prediction system for the North Atlantic European coastal Zones
TOPEX	TOPography EXperiment, part of the TOPEX/Poseidon satellite(joint radar altimetry project, NASA and CNES)
TWS	Total Water Storage
UK	United Kingdom
UoR	University of Reading
v0, v1	version 0/1 data set within SLBC_cci project
VM	model of the radial viscoelastic structure of the Earth (used fo ICE-5G)
WCRP	World Climate Research Programme
WFDEI	Watch Forcing Data based on ERA-Interim reanalysis
WGMS	World Glacier Monitoring Service
WP	Work Package
XBT	Expendable Bathythermograph
XCTD	Expendable Conductivity/Temperature and Depth

1 Introduction

1.1 Purpose and Scope

This document discusses the results of the sea level budget closure assessment at the intermediate stage of the project. Comparisons and results are based on version 1 (v1) data as they are described in detail in the SLBC_cci Product Description Document D2.3.2 (see below), or are indicated individually otherwise. v1 data and products have been developed and gathered during the WP2x2 phase of the SLBC_cci project. They were improved over version 0 (v0), which reflected the situation at the beginning of the project, prior to any improvement and further adaptation. The results were discussed within the entire consortium during the project meeting in October 2018, at monthly telecons and in numerous bilateral discussions.

Changes and adaptations in datasets from contributing WPs lead to several changes and improvements as follows:

- Longer time-series (to end of 2015 vs 2014 in v0)
- OMC improved, CMC included ('continental' mass change, without Greenland & Antarctica)
- Glaciers temporal resolution changed from yearly to monthly
- GMB for GIS updated; radar- and lidar altimetry now considered as well
- GMB for AIS updated; radar altimetry now considered as well, incl Antarctic Peninsula
- Land water storage ends now Dec 2015; i.e. +1yr compared to v0 analysis; new parameters included in the model, e.g. glacier mass change.
- Improved uncertainty assessment and documentation

Relevant documents:

SLBC_cci Product Description Document D2.3.2:

Novotny, K.; Horwath, M.; Cazenave, A.; Palanisamy, H.; Marzeion, B.; Paul, F.; Döll, P.; Cáceres, D.; Hogg, A.; Shepherd, A.; Otosaka, I.; Forsberg, R.; Barletta, V.R.; Andersen, O.B.; Ranndal, H.; Johannessen, J.; Nilsen, J.E.; Gutknecht, B.D.; Merchant, Ch.J.; MacIntosh, C.R.; Old, Ch.; von Schuckmann, K.: *ESA Climate Change Initiative (CCI) Sea Level Budget Closure (SLBC_cci). Product Description Document D2.3.2: Version 1 data sets and uncertainty assessments. Version 1.1, 25 Oct 2018.*

1.2 Document Structure

Chapter 2 discusses the global ocean mass budget as part of the global mean sea level (GMSL) change. Within this chapter, sources of ocean mass change (glaciers, ice sheets and hydrology) are compared to observed ocean mass changes. The subsequent Chapter 3 puts the GMSL into focus by looking at the mass and the steric component in GMSL change. Chapter 4 discusses the budget of the Arctic Ocean. The appendix shows a preliminary comparison of GRACE-based and model-based results on the sum of land water and glacier changes on land (other than Antarctica and Greenland).

1.3 Scientific Background

Sea level change, one of the best indicators of climate change, integrates the response of several components of the Earth system (ocean, atmosphere, cryosphere and hydrosphere) to anthropogenic and natural forcing. Studying the sea level budget helps to better understand processes at work and follow temporal changes (e.g., acceleration) of individual components. It increases our understanding on uncertainties of different observing systems and models. It also allows placing bounds on poorly known contributions (e.g., deep >2000 m ocean warming, not measured by current observing systems), constraining current Earth's energy imbalance and validating climate models used for simulating future climate. GMSL change as a function of time t is usually expressed by the sea level budget equation:

$$\Delta SL(t) = \Delta M_{Ocean}(t) + \Delta SSL(t) \qquad \text{[Eq. 1]}$$

where $\Delta SL(t)$ refers to the change in sea level, $\Delta M_{Ocean}(t)$ refers to the change in mass of the oceans and $\Delta SSL(t)$ refers to the steric contributions, namely the sum of ocean thermal expansion and the halosteric contribution, where in a global mean, the latter is zero due to global salinity conservation.

A major proportion of sea level change is due to the fact that water masses from land get re-distributed into the global ocean. The main sources are known to be melting glaciers and polar ice sheets, but also the variability in the onshore water masses budget has significant impact on sea level changes.

The ocean mass budget reads

$$\Delta M_{Ocean}(t) = - [\Delta M_{Glaciers}(t) + \Delta M_{GIS}(t) + \Delta M_{AIS}(t) + \Delta M_{LWS}(t) + \text{other}], \qquad \text{[Eq. 2]}$$

where $\Delta M_{Glaciers}(t)$, $\Delta M_{GIS}(t)$, $\Delta M_{AIS}(t)$ and $\Delta M_{LWS}(t)$ are the temporal changes in mass of glaciers, Greenland (GIS) / Antarctica (AIS) ice sheets and total land water storage (LWS), including seasonal snow cover. Other terms (e.g., atmospheric water vapour variability) were not considered in this assessment. The mass budget misclosure, as used in this report, is

$$\text{misclosure} = \Delta M_{Ocean}(t) + [\Delta M_{Glaciers}(t) + \Delta M_{GIS}(t) + \Delta M_{AIS}(t) + \Delta M_{LWS}(t)], \qquad \text{[Eq. 3]}$$

where the terms on the right-hand side in Equation 3 now are the assessed mass changes of the respective components, including their errors.

2 Ocean Mass Budget

2.1 Data update

For this chapter of the report, we used twelve different GRACE-based solutions with observed mass changes over the global ocean. These products and the contributing terms of the named components on the right side of Equation 2 in the previous section are taken from the SLBC_cci version 1 data pool as described in the Product Description Document D2.3.2.

"Other terms" according to Equation 2 (e.g., atmospheric water vapour variability) were not considered in this assessment.

WP222 Ocean mass change from GRACE (see Figure 2.1). Ocean mass time-series from twelve solutions as described in D2.3.2 were used:

- "WP222 Main product" ITSG-Grace2016 spherical-harmonics based solution, with GIA correction both after A et al. (2013) and Caron et al. (2018); globally integrated, buffered and scaled time series.
- CSR-, GFZ- and JPL spherical-harmonics based solution, each with both A et al. (2013) and Caron et al. (2018) GIA correction; identical method to the 'main product'; globally integrated, buffered and scaled time series.
- One mascon solution by the Goddard Space Flight Center (GSFC, Luthcke et al., 2013) dedicated for ocean mass research; globally integrated and scaled geodesic grid product.
- Chambers' OMC time-series for CSR, GFZ and JPL; spherical-harmonics based, globally integrated, buffered and scaled time series (Johnson and Chambers 2013, updated).

We have rescaled the obtained mass changes onto a common global ocean area of 3.61e+14 m^2. Different from version 0, we categorised the twelve solutions into four classes of similar origin. In a simple ensemble-mean approach taking into account all twelve provided OMC solutions equally, the higher number of self-produced OMC solution would inherently have higher weight and would distort a preferably even distribution of probe types. The advantage of performing a class-mean budget assessment instead is a fairer weighting between the classes.

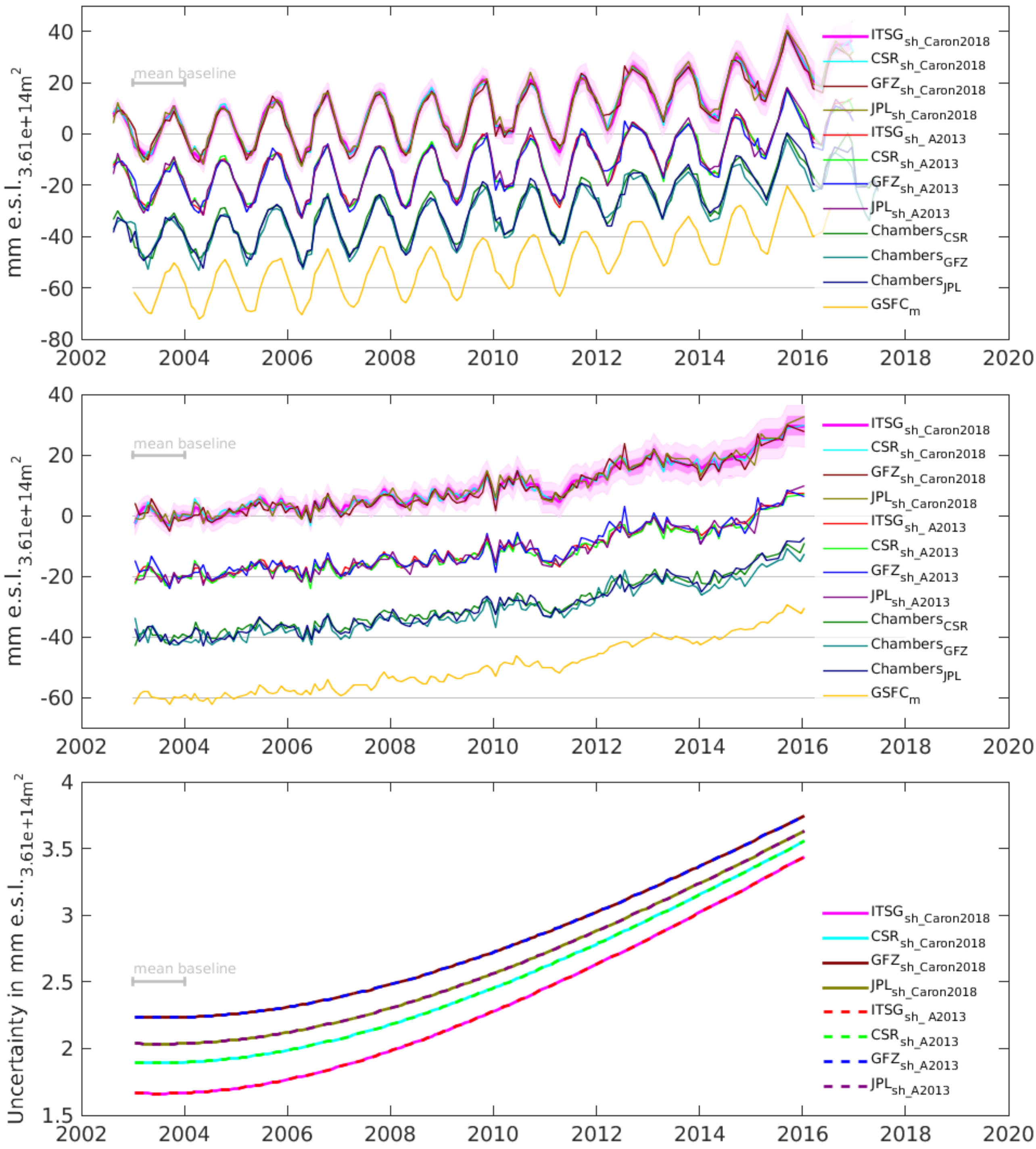

Figure 2.1: Top: GRACE ocean mass change (OMC). Magenta coloured uncertainty bands show the 1-sigma (cf. bottom plot) and 2-sigma range, respectively. All OMC data are plotted with respect to their 2003 mean ('mean baseline'). The single solutions are split into four classes as described in the text and shifted by -20 mm/yr per class for reasons of clearness. Centre: Same GRACE OMC as above but with seasonal signals (annual and semi-annual sine and cosine) removed and restricted to the assessment years 2003-2015. Bottom: 1-sigma standard uncertainties of changes w.r.t. the mid of the year 2003. Note how the uncertainty near the reference year is dominated by the solution's individual noise level, and how the uncertainty increases due to common trend uncertainty components (i.e. Deg1, C20, GIA, leakage) with distance in time relative to the reference time, which is the mean of the baseline (here: 2003.5).

The four classes were arranged as follows:

- **SLBC_SH_GiaC:** 4 self-produced OMC time series based on ITSG-Grace2016, CSR RL05, GFZ RL05a and JPL RL05 solutions (spherical harmonics) with GIA correction after Caron et al. (2018) applied.
- **SLBC_SH_GiaA**: 4 self-produced OMC time series based on ITSG-Grace2016, CSR RL05, GFZ RL05a and JPL RL05 solutions (spherical harmonics) with GIA correction after A et al. (2013) applied.
- **SH_Chamb:** An ensemble of three solution based on CSR RL05, GFZ RL05a and JPL RL05 by Don Chambers, spherical harmonics, GIA after A et al. (2013).
- **Mascon_GSFC:** One single mascon solution by GSFC.

While the model by A et al. (2013) is based on the ICE-5G deglaciation history, the GIA solution by Caron et al. (2018) is based on ICE-6G, which is an update of ICE-5G. While the model by A et al. (2013) is a single GIA model, the solution by Caron et al. (2018) arises from a large ensemble of models, where the glaciation history and the solid Earth rheology have been varied and tested against independent geodetic data to provide probabilistic information. This probabilistic information was used to calculate a weighted mean of the individual GIA models, which is what we call the "Caron et al. 2018 solution". We use Caron et al. (2018) for the GIA correction in our 'main product' because as compared to the model by A et al. (2013) it uses an updated glaciation model and a more comprehensive approach of analysing a whole ensemble of GIA models.

WP232 Glacier mass change (see Figure 2.2): Integrated mass change time series with now monthly resolution based on SLBC_cci v1 gridded data as documented in the Product Description Document D2.3.2. Uncertainties were originally given as half width of the 90 percent confidence interval. To convert them to standard uncertainties (standard deviation of the error), here the numbers were divided by 1.645, based on the assumption of a normal distribution of the errors. The determination of trend uncertainties is based on a data update of glaciers loss rates and rate uncertainties with annual resolution provided in late September 2018.

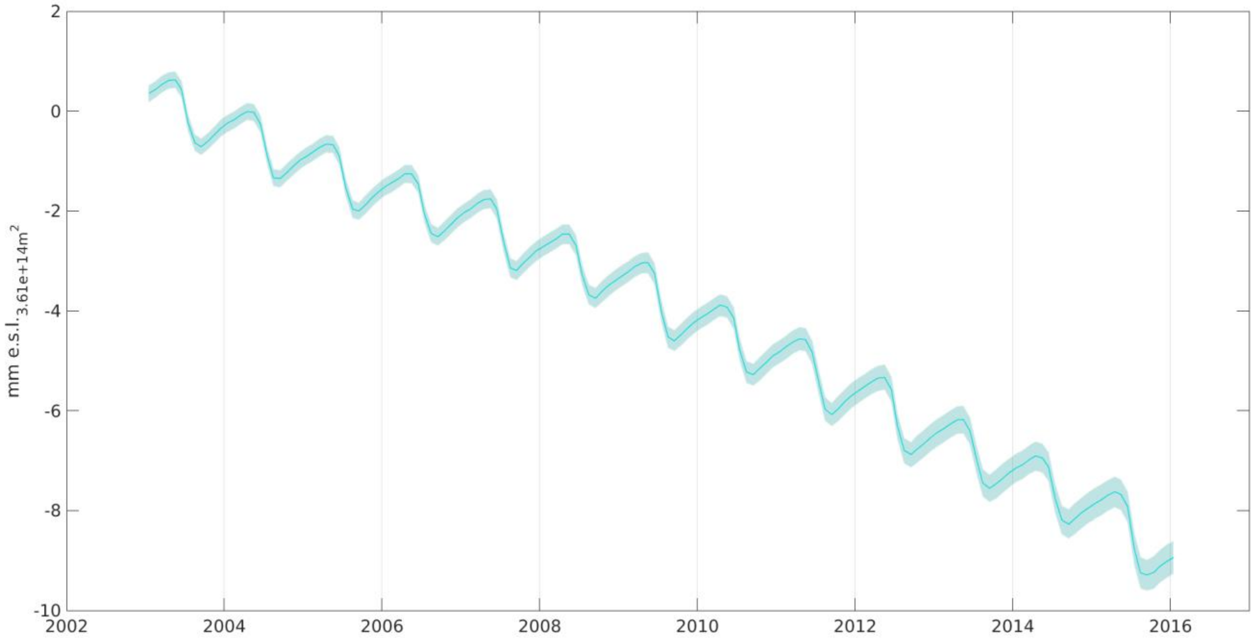

Figure 2.2: Glaciers mass change and uncertainties w.r.t. the year 2003 mean. The negative trend means net mass loss of the glaciers, i.e. mass gain for the Global Ocean.

WP242 Ice sheets mass change (see Figure 2.3 and Figure 2.4):

- GIS:
  - GMB integrated mass change time-series for entire Greenland (GIS00_grace.dat) as documented in the Product Description Document D2.3.2. Uncertainties of the trends were taken from Table 6.2 of D2.3.2. The expected range of accuracy errors of 9 Gt/yr given there translates into 0.025 mm/yr sea level (throughout this chapter we count 1 Gt land water or land ice to correspond to 1/361 mm equivalent sea level) and is plotted in Figure 2.3 as purple uncertainty band with respect to 2003.
    An error of the linear fit to the time series is not considered in this value. A noise component for this time series is yet to be determined.
  - Lidar altimetry (one linear trend for 2003-2009; red dashed line in Figure 2.3)
  - Radar altimetry, given as annual rates and plotted as cumulative change with respect to 2003 in Figure 2.3 (black curve). The volume change underlying these data is expected to underestimate the actual change as the method is restricted to slopes less than 1.5 degrees.

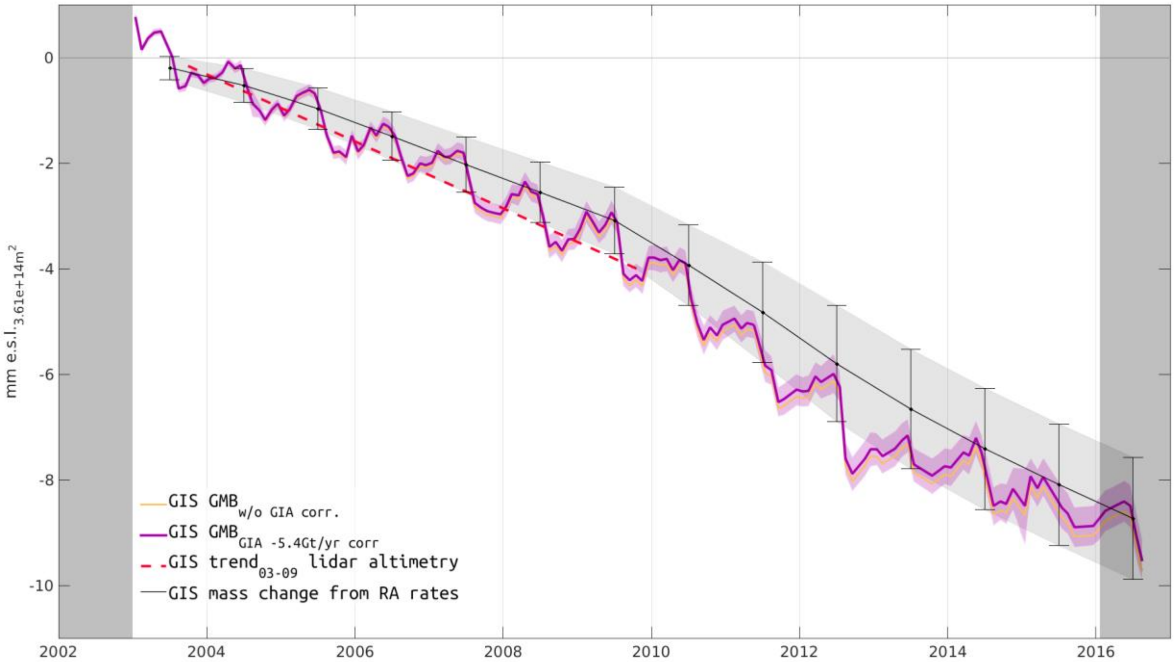

Figure 2.3: Greenland Ice Sheet (GIS) mass change from different sources: GMB (purple, with 1-sigma uncertainty band), lidar altimetry (red dashed line, one single linear trend 03-09) and radar altimetry (black). Note that radar altimetry may underestimate volume change, as slopes greater 1.5 degrees (at the GIS margin) are not well resolved. A negative trend means GIS net loss, i.e. gain for the Global Ocean.

- AIS:
  - GMB integrated mass change time series for entire Antarctica (AIS_GMB_basin.dat, AIS32) as documented in the Product Description Document D2.3.2. Uncertainties of the trends were taken from Table 6.3 of D2.3.2 and from an additional data file provided with v1 (AIS_GMB_trend.dat).
  - Radar Altimetry, now also including the Antarctic Peninsula.
  - Note that discrepancies between altimetry-based and GRACE-based mass change estimates exist for the EAIS (Figure 2.4). They have been observed previously and are not well understood. See, e.g., Shepherd et al. (2018); Schröder et al. (2019). Possible causes are: errors in the GRACE GIA correction, time-variable penetration effects on radar altimetry; imperfect altimetry inter-mission calibration, imperfect altimetry volume-to-mass conversion. Note that the visual perception that deviation starts after 2009 is due to the arbitrary vertical shift of the two time series. More generally, the discrepancy seems to be a combination of a difference in the trends and a difference in the representation of events like the 2009 jump visible in the GRACE time series.

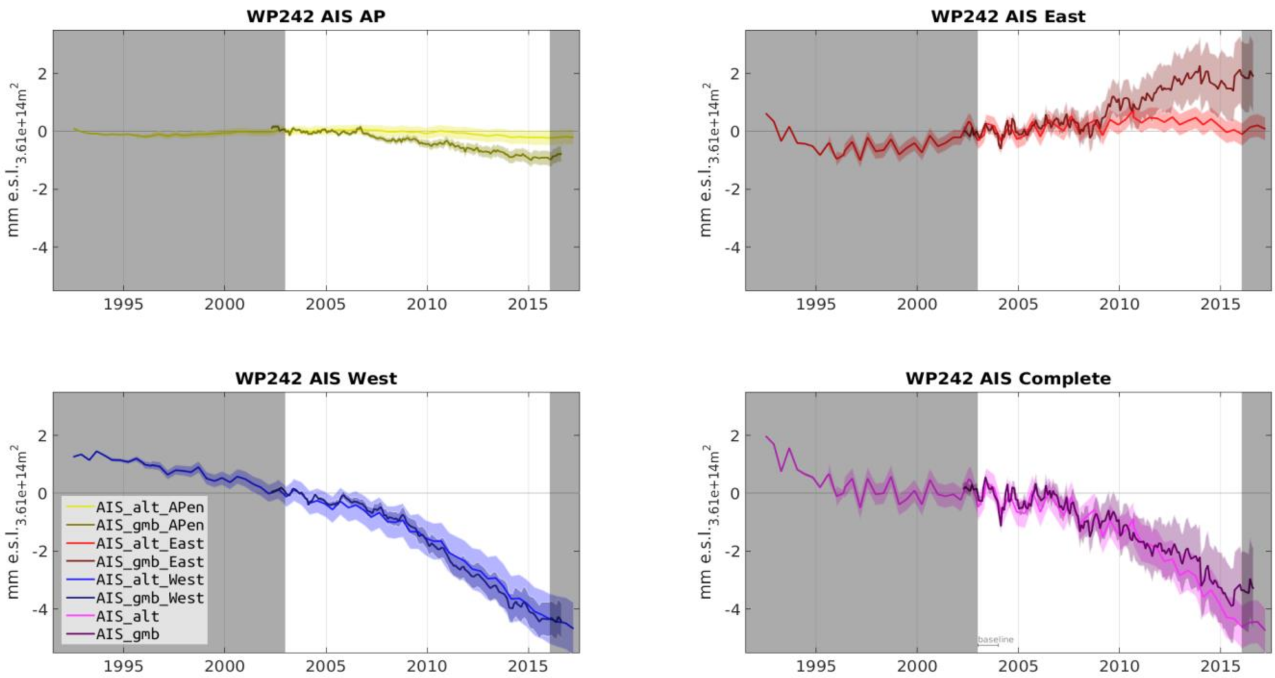

Figure 2.4: Antarctic Ice Sheet mass change relative to the 2003 mean. All four panels show the GMB and altimetry solutions, respectively. Top left: Antarctic Peninsula; top right: East Antarctica; bottom left: West Antarctica; bottom right: Combined Antarctica. The reference time for the GMB uncertainty bands is mid of 2003. For the altimetry, the reference time is at the start of the time series in 1992. Negative trends correspond to as mass gain for the Global Ocean.

WP252 Land water mass change (see Figure 2.5): CRU- and WFDEI/CRU-driven globally integrated monthly time series of equivalent water heights (tws_WaterGap22c[...].txt) with irrigation scenarios 70 and 100 as documented in the Product Description Document D2.3.2, rescaled from source area to ocean area. Given monthly time stamps were treated as mid-of-month (representing the mass change of each month, respectively). For the land water contribution, no uncertainty assessment is directly available. We have chosen to estimate the uncertainty of the multi-year trend according to the standard deviation of the ensemble-member trends.

The following SLBC_cci v1 available data have not been considered in this mass budget assessment:

- WP252 Land water storage: Data based on WFDEI-GPCC with irrigation scenarios 70 and 100 end with Dec 2013 and were not considered in the common assessment due to consistency reasons with other data sets (the SLBC_cci v1 mass budget assessment time-frame is 2003-2015). It should be noted that these two model runs show less net loss over the common period (compare green and light-blue curve in Figure 2.5) and would presumably decrease the contribution to the sum-of-components, but increase the mean variation of the ensemble trend if available at the full time span.

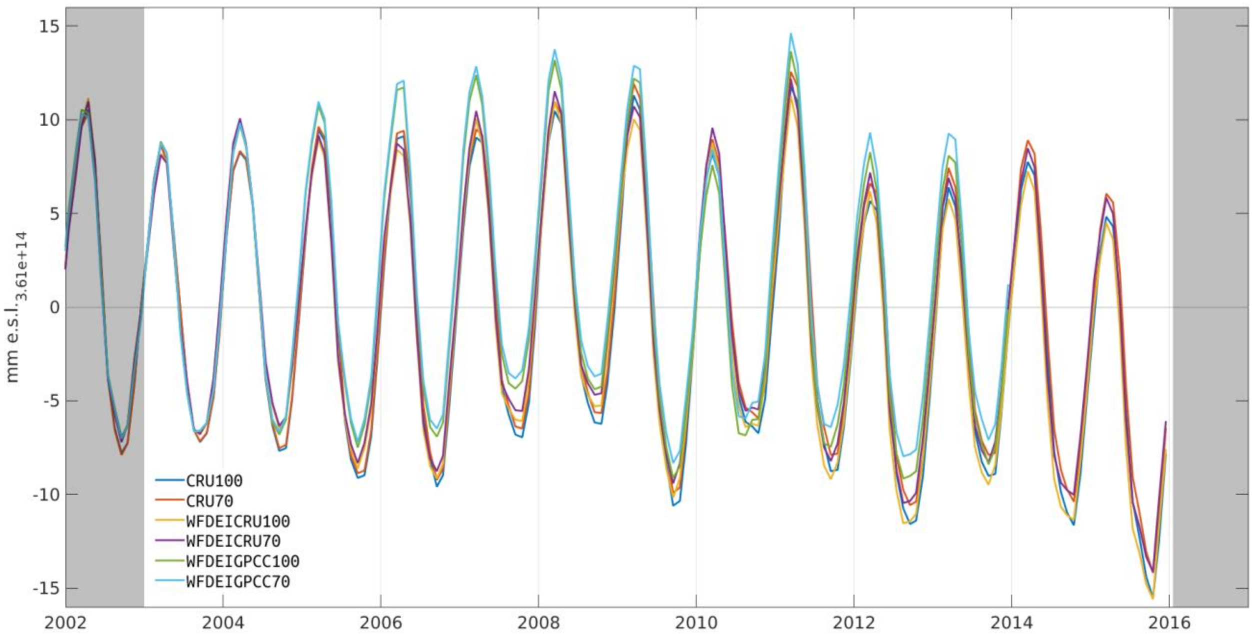

Figure 2.5: Land water storage change w.r.t. the year 2003 mean, with negative trends meaning net mass loss off the continents. Note the large seasonal variation in amplitude. The WFDEI/GPCC type is missing the years 2014-2015 and was not further considered. The four CRU- and WFDEI/CRU-type series cover the entire SLBC_cci period and an ensemble mean of them was applied throughout the version 1 assessment.

2.2 Budget assessment

2.2.1 Methods

The time series of contributing components were considered over a common time interval from 01/2003 to 12/2015, which is an additional 12 month period over the v0 assessment. GRACE time-series are lacking data in the last 2-3 months of 2015, after only partial Level-1B data was delivered between end of 9/2015 and mid of 12/2015. Therefore, one additional month (Jan 2016) was included for SLBC_cci version 1 trend determination as a supporting end-node for interpolation (see below).

Version 1 data, that were given as gridded mass changes over land were globally integrated and scaled onto a common standard ocean surface area of 3.61e+14 m².

An un-weighted least squares fit of a 6-parameter function (consisting of a constant, a linear component, an annual cosine and sine function and a semi-annual cosine and sine function) was computed for each restricted mass change time-series based on un-interpolated data, respectively. The linear component of this functional fit is treated as the "trend" and is expressed in units of Gt/yr (gigatonnes per year) for the OMC trend and in mm/yr (millimetres per year) for an equivalent sea level change that corresponds to the OMC. This trend is used for assessing the ocean mass budget. Data with annual temporal resolution (GIS altimetry) were fitted with the same function but without adjusting for annual and semi-annual components.

Uncertainties of the trends are taken from D2.3.2, with the addition of one update [26-Sep-2018] of gridded uncertainties of annual glacier mass loss rates. They are considered as standard uncertainties (standard deviation of the error, "one sigma"). Note that these uncertainties exceed the formal uncertainties of the functional fit because their assessment includes systematic effects (e.g. GIA uncertainty, in the case of GRACE-based data products). Uncertainties of sums or differences of the trends from individual contributions are taken as the root sum square of the individual uncertainties. For an assessment on the land water mass trends, we considered the spread between the linear trends obtained from the four land water mass time series that cover the full period 2003-2015. A comparison to the restricted period of all six series until end of 2013 (cf. Figure 2.5) indicates that including the WFDEI/GPCC type could result in a less negative ensemble trend in the LWS component and, thus, in the sum of components.

Wherever possible in terms of the provided v1 data, we combine uncertainties in the form

$$\sigma_{total}^2(t) = \sigma_{noise}^2(t) + (\sigma_{trend}\cdot(t-t_0))^2$$

for time series of mass change m(t)-m(t_o) with respect to a reference time t_o. This means, the uncertainty range at the reference time is σ_{noise} and increases in time before and after the reference time, e.g. compare Figure 2.1. By applying this method, we take care of the fact that mass change comparison plots are often mis-interpreted as they seemingly diverge more in certain years than in others, when they indeed only are plotted with respect to the mean of a reference year and thus inherently show smaller and greater differences at different years, respectively.

The mass budget was derived from the linear components of (a) ocean mass change and (b) the sum of components, namely Glaciers, AIS, GIS and LWS (cf. Equation 2 and 3). We generated two other sets of time series for purposes of displaying and of analysing the non-linear and non-seasonal components:

- In one set of time series we reduced the annual and semi-annual components.
- In another set of time series we additionally reduced the linear component (trend).

In addition, we then interpolated those time series to a common mid-monthly temporal sampling from 01/2003 to 12/2015. For GRACE OMC, the month of 1/2016 served as an additional sampling node in order to support the missing months of Q4/2015, avoiding extrapolation. Interpolation is necessary for comparative analyses because of the inhomogeneous time basis of the underlying data products. Based on the common temporal sampling, we calculated the misclosure of the non-linear, non-seasonal components and analysed it statistically. However, the *trends* and analysis of *annual signals* considered throughout this assessment are solely based on original, un-interpolated time series. The same holds true for the evaluation of seasonal amplitudes, which is solely based on analyses of data at original times.

2.2.2 Results for linear trends

The linear trends for all considered terms of the ocean mass budget are given in Table 2.1. For the time interval 2003–2015, all considered components show a clear positive trend (with positive meaning mass loss on land):

- The **sum of components** is **2.052 +/-0.134 mm/yr** for 2003–2015, where the given uncertainty is the root sum square of individual component uncertainties and an LWS ensemble mean is applied; GMB results are used for both ice sheets.
- The **Greenland Ice Sheet** has the **largest contribution by 0.746 +/-0.025 mm/yr** from GRACE GMB (including peripheral glaciers) and **0.692** mm/yr assessed from radar altimetry (excluding peripheral glaciers and steep-slope areas).
- The WP232 **glaciers** contribute with **0.700 +/-0.013 mm/yr**.
- The combined **Antarctic Ice Sheet's** contribution from **GMB** is **0.273 +/-0.104 mm/yr**. The corresponding trend derived from **altimetry** is **0.321 mm/yr**.
- The trend in **land water storage** for four considered model variants has changed considerably compared to the v0 assessment. It now ranges now from 0.24 to 0.43 mm/yr, while it was 0.11-0.18 mm/yr for 2003-14 in v0. The **ensemble mean is 0.332 mm/yr**. This increase is the main cause for the increased sum-of-components trend compared to v0. The increase in the LWS trend from v0 to v1 has two reasons: First, the new v1 model versions generally have larger negative trends than v0, even for the commone period 2003-2014. Due to LWS changes occuring in 2015, the longer period 2003-2015 generally exhibits a larger negative trend than the shorter period 2003-2014. . An LWS ensemble mean is applied for the subsequent budget assessment. The uncertainty of the LWS trend is **+/-0.080 mm/yr** based on the "ensemble spread approach" (see Novotny et al. 2018, Section 2.2.1; Dieng et al. 2017, Section 2). Further analysis and more diverse spreads over the full SLBC_cci period may help to strengthen the solidness of the LWS uncertainty value.

The misclosure of the trend for the common period 2003–2015 is -0.141 mm/yr when an ensemble mean of all twelve GRACE-based solutions is considered. The spread between the misclosures resulting from the twelve different GRACE OMC series has a standard deviation of 0.163 mm/yr.

Our preferred GRACE SH OMC solution based on **ITSG-Grace2016 data with Caron et al. (2018) GIA correction** shows an average linear trend of **+1.918 +/-0.240 mm/yr** which results in an **OMC budget closure of -0.133 +/-0.275 mm/yr**, i.e. the budget is clearly closed within 1 standard uncertainty.

Details about the dependence of the misclosure on the used GRACE OMC dataset are given in Table 2.2 and Table 2.3. An LWS ensemble mean was applied throughout this analysis. The mean misclosure of all four classes is -0.084 mm/yr. Omitting the SLBC_SH_GiaA class leads to a mean class misclosure of -0.003 mm/yr. The self-produced SH-classes give a slightly lower trend (-0.33/-0.13 mm/yr) than the sum of components, while the trends of the mascon- and Chamber classes are marginally higher (+0.11/+0.01 mm/yr). The smallest single mass budget misclosure for the linear OMC trend in the period 2003–2015 can be found for Chambers CSR (+0.023 mm/yr), while in the SLBC_SH_GiaC class it was found for the JPL solution (-0.097 mm/yr). The SLBC_SH_GiaA class has a systematically more negative misclosure, which is attributed to the different GIA model: The GIA correction after Caron et al. (2018) leads to a stronger OMC trend by +0.2 mm/yr compared to the correction after A et al. (2013).

The fact that the SH_Chamb class solutions offer a higher trend than the SLBC_SH_GiaC class, despite the use of the lower-trending A et al. (2013) GIA correction, may be the result of a different integration area during GAD background model restoration and mean atmospheric pressure removal over the Global Ocean. In our analysis for D2.3.2 we found that the (correct) consideration of background models over the *entire* Global Ocean leads to *weaker* OMC trends than over the (coastal-)buffered and re-scaled ocean only. See Data Description Document D2.3.2 and Uebbing et al. (2018, in review) for details.

The observed spread of trends owing to different geodetic and geophysical corrections during the generation of our SLBC_cci v1 OMC time-series has demonstrated how easily a 'lucky' combination of wrong/insufficient corrections terms and methods may lead to trend values that match the observed sum of components. The SLBC_SH_GiaC class members of version 1, on the contrary, comprise the best understood and the most trusted and tested corrections at the time of processing. Out of these, the ITSG-Grace2016 based OMC data are known to have the lowest noise level (cf. Figure 2.1 bottom) and are thus entitled the SLBC_cci WP222 'main product'.

Table 2.1: Linear trends of contributing components and sum of components in SLBC_cci v1.

	Trend 2003-2015 mm/yr	**Uncertainty 2003-2015 mm/yr**
WP232 Glaciers	-0.700	+/-0.013
WP242 GIS (mean) {GMB, Altimetry$_{LinearFit}$}	-0.719 {-0.746, -0.692}	+/-XXX +/-{0.025, XXX}
WP242 AIS (mean) {GMB, Altimetry}	-0.297 {-0.273, -0.321}	+/-X.XXX +/-{0.104, XXX}
WP252 LWS (ensemble mean) {CRU100/70, WFDEICRU100/70}	-0.332 {-0.345, -0.238, -0.431, -0.315}	+/-0.080
Sum of components (GMB,LWS$_{ens}$) min / max (all available components)	**-2.052** (-1.903 / -2.198)	**+/-0.134**
Sum of comp. with 'altimetry' / 'GMB-altimetry mean' over ice sheets	-2.045 / -2.048	

2.2.3 Results for time series with full temporal resolution

Figure 2.6 shows the comparison between the individual components, the sum of components, and the OMC on a monthly time series basis. In this figure, results are displayed for all data with seasonal signals still included. Ice sheet data in this analysis is restricted to GMB data as it is the only ice-sheet product in SLBC_cci v1 that offers quasi-monthly resolution.

Figure 2.7 concentrates the OMC series into classes of similar origin (processing) while the fit to the seasonal signal was removed. The LWS time series is fixed to the same LWS ensemble mean as before.

Figure 2.8 shows the misclosure for the four individual LWS time series. Here, the GRACE OMC time series is fixed to the ITSG-Grace2016 based solution with GIA correction after Caron et al. (2013). While the LWS trends differ notably, they all match the OMC reference curve within uncertainties when combined with the trends of the other contributing components (compare values in Tables 2.1 and 2.2).

In addition to looking at the misclosure in terms of linear trends, we further analyse the misclosure on a time series level statistically.

Table 2.2: Linear trends 2003-2015 of different GRACE OMC solutions in SLBC_cci v1 and their misclosure with the sum-of-components (using GMB estimates for ice sheets and the model ensemble estimate for LWS).

	Trend 2003-2015 mm/yr	**Uncertainty 2003-2015 mm/yr**
1/2: ITSG-GRACE2016 sh (A/**Caron**)	+1.720 / **+1.918**	**+/-0.240**
3: GSFC RL5 mascon	+2.161	t.b.d.
4/5: CSR RL5 sh (A/Caron)	+1.696 / +1.894	+/-0.240
6/7: GFZ RL5a sh (A/Caron)	+1.719 / +1.917	+/-0.240
8/9: JPL RL5 sh (A/Caron)	+1.756 / +1.955	+/-0.240
13: Johnson & Chambers ensemble 10-12: {CSR, GFZ, JPL}	+2.065 +{2.075, 1.985, 2.135}	
OMC [1:12] **{[1:2] [3] [4:9] [13]}** **{[1:2] [4:9]}** **A([1 4 6 8]) / Caron([2 5 7 9])**	+1.911 {+1.967} {+1.822} (+1.723) / (+1.921)	
Trend Misclosure (ITSG, Caron, GMB, LWSens) Trend Misclosure [1:12] (same combinations as above)	**-0.133** -0.141 {-0.085} {-0.230} (-0.329) / (-0.130)	**+/-0.275** applies to solutions [1-2,4-9]

Table 2.4 shows the standard deviations (STD) of the monthly resolution time series of misclosure for the different GRACE-based ocean mass change products. The statistics are shown for (a) the full time series, (b) the time series after removal of the seasonal signal (from the annual and semi-annual sinusoidal fit), and (c) after removal of the seasonal signal and the linear trend.

Table 2.3: Misclosure of linear trends 2003-2015 between different GRACE OMC classes with sum-of-components in SLBC_cci v1 (LWS ensemble, GMB for ice sheets)

GRACE OMC CLASSES	Misclosure (GMB,LWS_{ens}) mm/yr	Misclosure Combined Uncertainty mm/yr
SLBC_SH_GiaA	-0.329	+/-0.275
SLBC_SH_GiaC	-0.130	+/-0.275
SH_Chamb	+0.013	
Mascon_GSFC	+0.109	
Class ensemble mean (all 4 classes)	-0.084	
Class ensemble mean without SLBC_SH_GiaA ("3-class-mean")	-0.003	

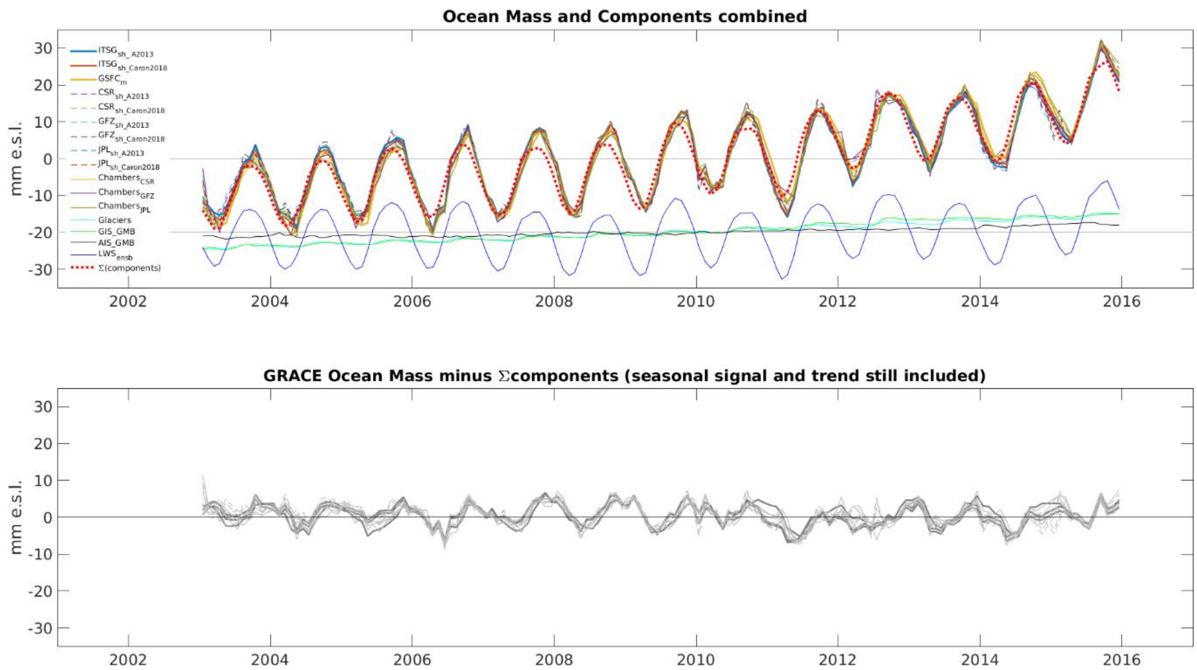

Figure 2.6: Ocean mass components with seasonal signal still included; lower panel: misclosure.

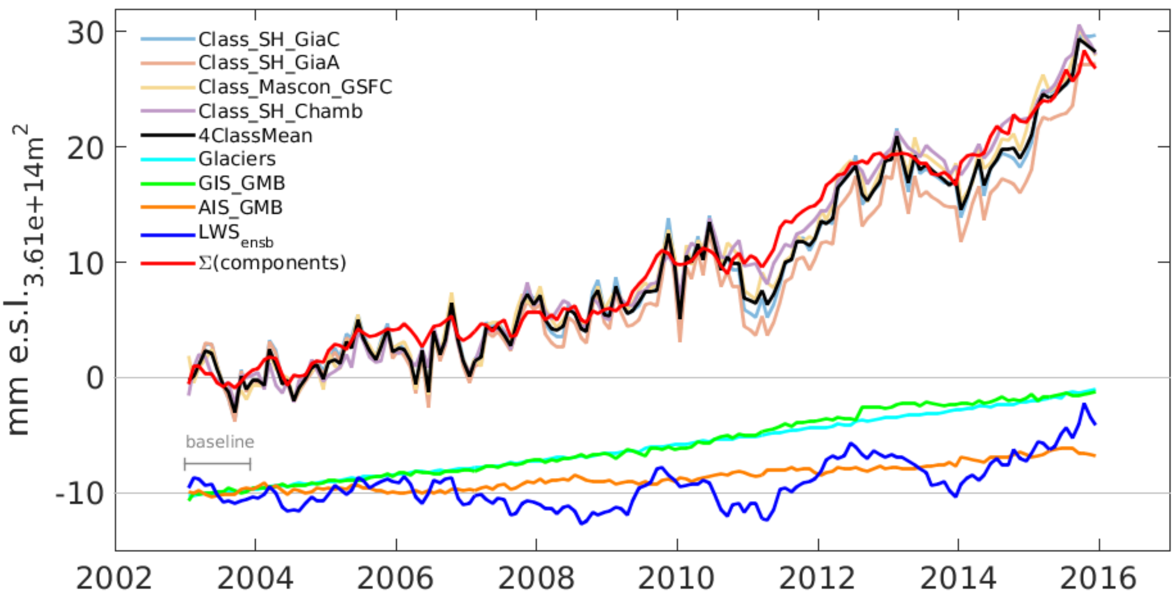

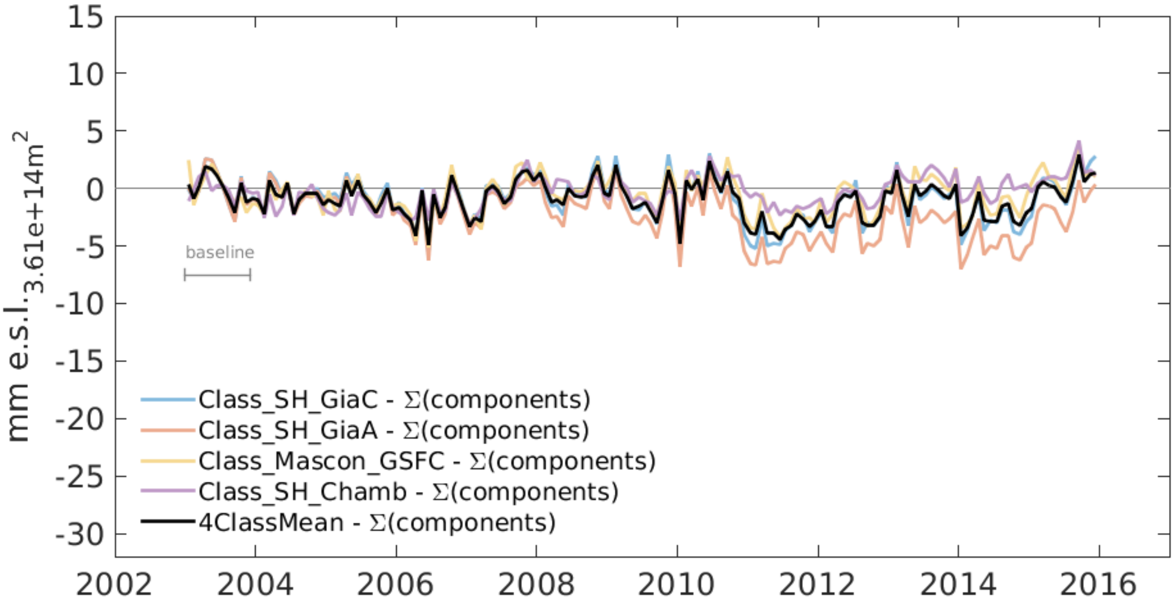

Figure 2.7: Top: Time series of individual components, OMC classes and sum of components (SOC, red) with respect to their 2003 mean ("baseline"). The seasonal signal is removed from each time series; interpolation to a common time sampling at mid-of-month was applied. The black line is the mean of the four faint-coloured classes. This SOC uses GRACE GMB for the ice sheets and an ensemble mean of land water storage. Bottom: Misclosure between OMC and SOC after the seasonal signal was removed from all time series.

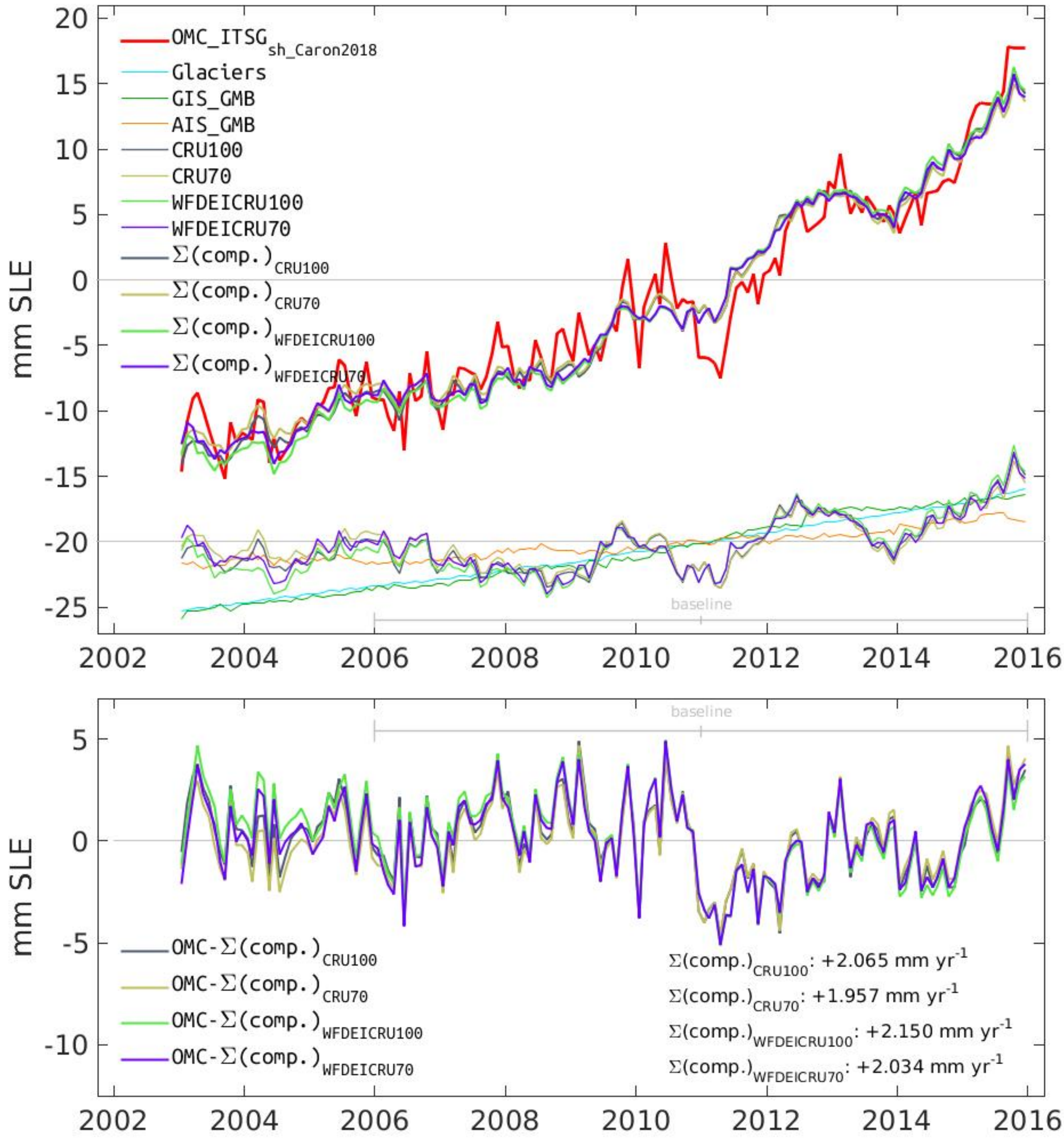

Figure 2.8: Sum of components with 4 different LWS model choices in comparison with ITSG-Grace2016 based OMC (red, GIA corrected after Caron et al., 2013). Annual and semi-annual signal are removed and data are shown relative to their 2006-2015 mean. The lower panel depicts the monthly misclosure, which is GRACE OMC minus sum of components. The numbers at the lower right are the sum-of-component trends with individual LWS solutions, respectively.

Table 2.4: Standard deviations of the monthly resolution time-series misclosure (2003–2015) for the different OMC solutions a) with included seasonal and linear components, b) after reduction of the seasonal signals and c) after additional reduction of the linear component.

STD of monthly misclosure	a) incl. trend and seas. comp. mm	b) seas. removed mm	c) seas. and trend removed mm
ITSG-GRACE2016 GiaA	2.91	2.16	1.90
ITSG-GRACE2016 GiaC	2.73	1.91	1.90
GSFC_m	2.91	1.35	1.26
CSRsh GiaA	2.94	2.35	2.05
CSRsh GiaC	2.73	2.08	2.05
GFZsh GiaA	3.10	2.54	2.30
GFZsh GiaC	2.91	2.32	2.30
JPLsh GiaA	3.06	2.50	2.33
JPLsh GiaC	2.92	2.33	2.33
Chambers CSR	2.72	1.70	1.69
Chambers GFZ	2.96	2.09	2.08
Chambers JPL	3.11	2.10	2.07
SLBC_SH_GiaA CLASS	3.01	2.39	2.14
SLBC_SH_GiaC CLASS	2.82	2.16	2.14
SH_Chamb CLASS	2.93	1.97	1.95
4 class mean	2.91	1.97	1.88
3 class mean	2.88	1.83	1.79

The STD of the misclosure decreases significantly by ~0.8 mm e.s.l. after removal of the seasonal components. This points to a misclosure of the seasonal components, which is the subject of ongoing investigations.

As can be seen in Table 2.4 and Figure 2.9 , the OMC from the GSFC mascon solution has low misclosure STDs only after removal of its seasonal signals, which show the largest deviation from those of the sum of components (cf. yellow and red arrows in Figure 2.9). Regarding the annual cosine and sine fit to the time-series, the SLBC_sh class v1 OMC products are closest to the sum of the contributing components. Annual signals in CRU landwater data appear to match the GRACE OMC solutions better than from CRU/WFDEI landwater solutions. The irrigation scenario (70 or 100) has no notable impact on the phase.

The STD of the misclosure decreases further after removal of the linear trends, but only by ~0.1 mm e.s.l. on average. While the trends of the Caron-corrected solutions fit very well to the SOC trend and consequently do not show much improvement, the A et al. GIA corrected solutions from SLBC_cci WP222 'improve' here a lot, since their trend is systematically lower than that of the SOC.

This observation by itself does *not* approve one GIA model as correct but the observed behaviour is strictly valid for the applied combination of all components and will change when different component-sources are applied. The choice of parameters, corrections and components as a whole determines a good closure in combination with the assessed uncertainties.

The STD of the misclosure in the non-linear and non-seasonal components indicates that GSFC mascons, Chambers_CSR and ITSG-Grace2016 (independent of GIA correction model) show the smallest mass budget misclosure for those temporal components. More details on the statistics of the misclosure of the non-linear, non-seasonal components are shown in Figure 2.11.

Figure 2.10 finally shows the misclosure time series contrasted to the uncertainty band of the GRACE OMC time series, which is part of (but does not yet comprise the entire) assessed uncertainty of the misclosure.

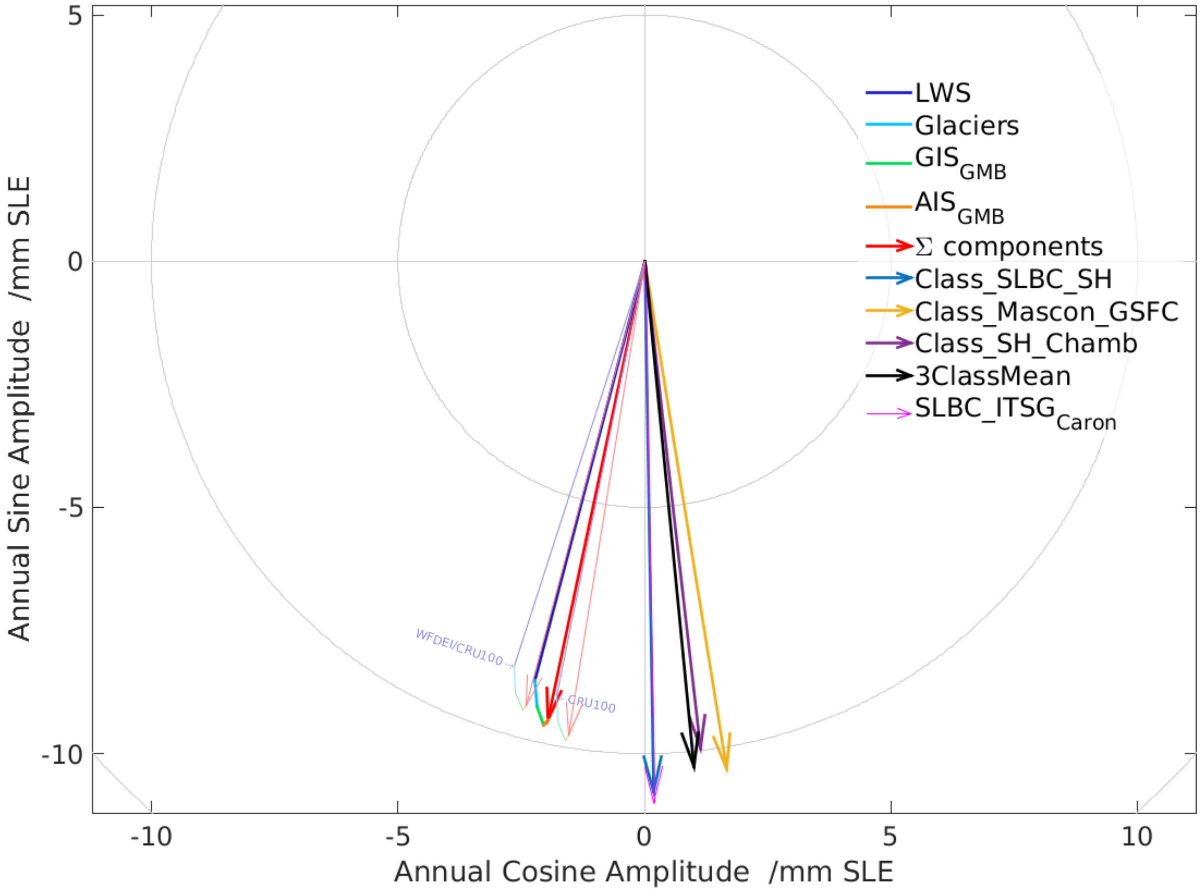

Figure 2.9: Cosine amplitudes versus sine amplitudes (x- and y-axis) of the annual fit to OMC and to the contributions from the contributing components. Note that the annual signal does not depend on the GIA correction. The bold red arrow depicts the vector sum with the LWS ensemble mean, while the faint red arrows show the same for individual LWS model runs.

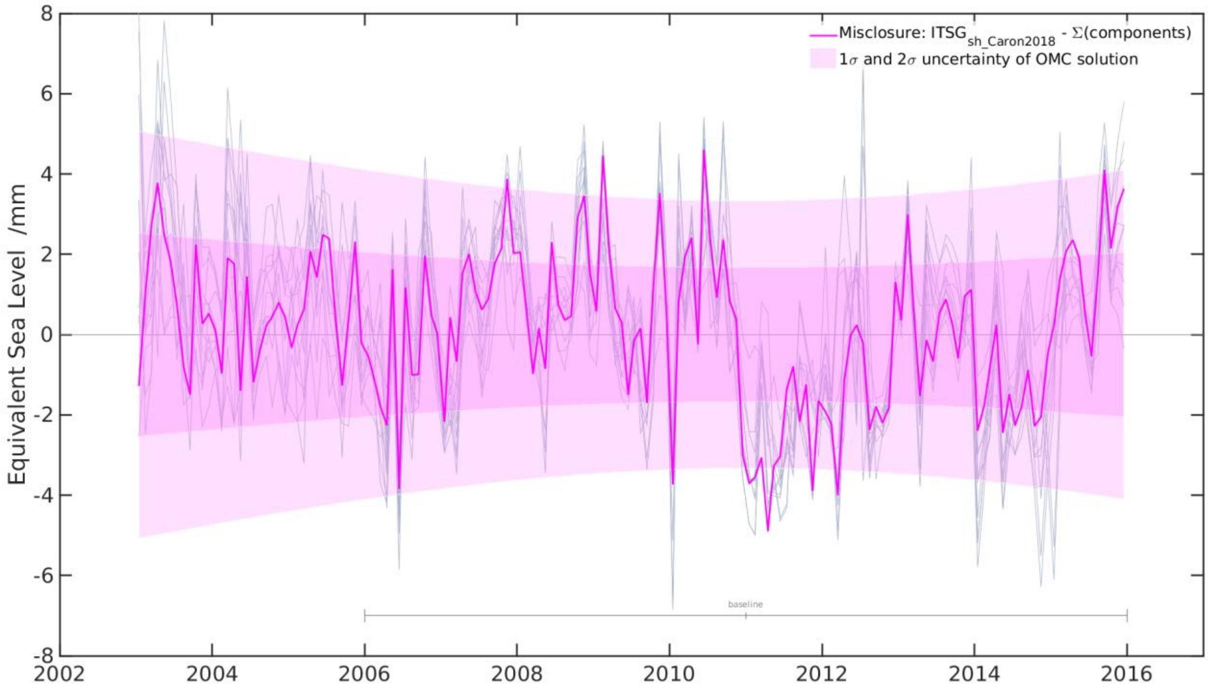

Figure 2.10: Misclosure time series based on the ITSG SH solution with GIA correction after Caron et al. 2018 for OMC, the ensemble mean for LWS and the GMB products the ice sheets (magenta curve). Grey curves shows the similar misclosure for all other GRACE OMC solutions. Also shown are the 1-sigma and 2-sigma bands of the GRACE OMC time series, which are part of the uncertainty of the misclosure time series but do not yet include the uncertainty contribution from the sum of components.

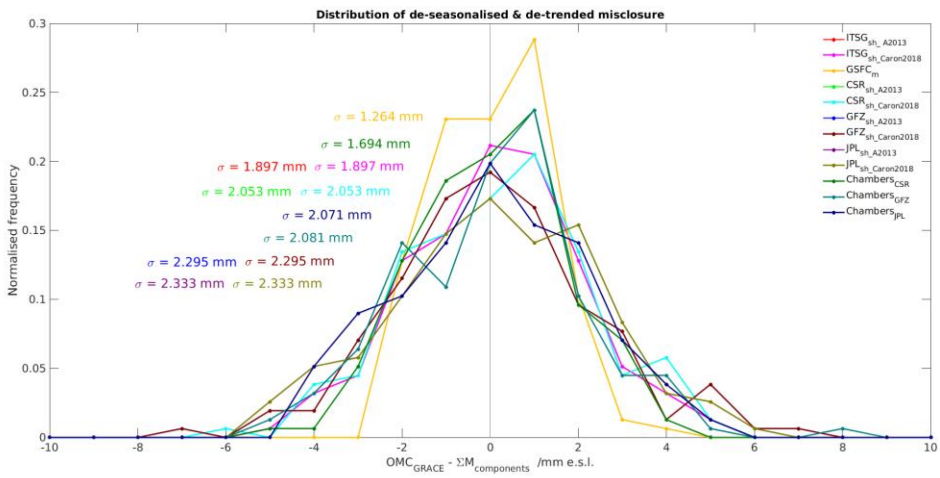

Figure 2.11: Distribution of misclosures after removal of seasonal and linear signals. Note that the curves of SLBC produced series with A et al. (2013) GIA correction are not visible as they exactly match the Caron et al. (2018) corrected data after removal of the trend.

2.3 Discussion and Conclusions

The misclosure of the linear trends over 2003-2015 is within the combined uncertainty of OMC and the sum of components. Hence, the ocean mass budget in terms of linear trends is closed within its uncertainty.

Time series including seasonal cycles show a considerably larger mismatch between the observed signal and the sum of contributing components. Time series from which the seasonal cycle has been removed show a considerably better budget closure.

Ongoing analyses of seasonal terms should give more insight into possible systematic mismatch or other causes. Especially the GSFC mascon solution stands out to closely match the sum of components after removal of seasonal signal on the one hand, but shows a comparably large deviation with the seasonal terms still included on the other hand.

In terms of the seasonal signal, the SLBC_SH classes, that is, the OMC solutions best understood by us, agree best with the sum of components from cryosphere and hydrosphere.

Noisier GRACE OMC solutions (e.g. GFZ, JPL) after removal of seasonal and linear signals show a tendency towards a larger misclosure (compare Table 2.4).

The assessment of trend uncertainties of the considered mass change components of land, cryosphere and ocean differ considerably. While the glacier and ice sheet mass change trend uncertainties are relatively well known in order to be considered, an equivalent for the trend in changes of land water masses is still to be determined. However, GRACE-based ocean mass time series still show larger (about twice of components) uncertainties and are partly not assessed by identical standards for several solutions (SH_Chamb and Mascon_GSFC classes).

3 Global Sea Level Budget

We assess the global mean sea level budget using the version 1 (v1) data provided by the project partners of the different components of the sea level budget. We first discuss each component individually, then analyze closure of the sea level budget over the two study periods.

3.1 Data update

We first analyze the individual SLBC_cci v1 sea level components and perform comparisons with other existing external sources such as data from WCRP (2018) and other recently published articles over the 1993-2015 period (wherever applicable) and/or over the period 2005-2015.

Detailed description of the v1 products are provided in the Product Description Document D2.3.2. The annual and semi-annual cycles were removed in all sea level components time series through a least-squares fit of 12-month and 6-month period sinusoids. No interpolation was performed to fill any existing data gaps in the time series. Linear trends were then estimated using the least squares fit methodology on the un-interpolated data without annual and semi-annual cycles.

For the products whose mass components and associated errors are provided in gigatons (Gt) per year, we converted them into mm of sea level equivalent (SLE) by dividing by a factor of 361 (taking into account that 361 Gt of ice mass would raise globally the mean sea level by 1 mm approximately). All results below are expressed in mm SLE.

Any other specific data processing is explained under the corresponding section.

3.1.1 Sea level

We used the CCI based Ablain et al. (2017) GMSL time series. This time series uses version 2.0 of the ESA Climate Change Initiative CCI 'Sea Level' project (SL_cci). These data combine observations from the TOPEX/Poseidon, Jason-1/2, GFO, ERS-1/2, Envisat, CryoSat-2 and SARAL/Altika missions averaged over 82°N and 82°S latitudinal range, and are available at a monthly resolution over 1993-2015. The TOPEX A drift correction between 1993 and beginning of 1999 from Ablain et al. (2017), that involves comparison of the altimetry-based sea level time series with tide gauges and then filters out the differences by applying a Lanczos low pass filter, has been applied to the CCI GMSL time series. Glacial Isostatic Adjustment (GIA) correction of -0.3 mm/yr based on Peltier (2004) has also been applied to this time series. Uncertainty estimation at each time step for GMSL time series is currently unavailable. Various processing groups provide GMSL trend uncertainty based on various geophysical corrections, instrumental drifts and other systematic errors and this account to ± 0.5 mm/yr with a confidence interval of 90%, thereby ± 0.3 mm/yr if we consider one sigma, in the case of CCI GMSL time series.

3.1.2 Individual mass components affecting sea level change

3.1.2.1 Ice sheets

(a) Antarctic Ice Sheet (AIS)

Two AIS mass change time series are available from the SLBC_cci v1 data base: (1) Altimetry based AIS mass change time series over 1992-2016 and (2) GRACE based AIS mass change time series over 2002-2016.

The altimetry based AIS mass change time series comprises data for the East Antarctic, West Antarctic and Antarctic Peninsula ice mass change derived from radar altimetry and a time evolving ice density mask. The mass change time series is derived from surface elevation change generated by processing Level 2 elevation measurements provided by ESA, and acquired by multiple radar altimetry satellite missions, ERS-1, ERS-2, Envisat and CryoSat-2. The available time series contain information on time, integrated cumulative mass balance and measurement uncertainty at a 140 days epoch. The uncertainty in mass change is estimated by summing in quadrature the uncertainty associated with our elevation change measurements (considering systematic errors, time-varying errors and errors associated with the calculation of inter-satellite biases) and the snowfall variability uncertainty to account for the additional error associated to the identification of ice dynamical imbalance. More information on data processing and uncertainty estimation is available in the Product Data Description Document D2.3.2. The v2 dataset will contain un-cumulated uncertainties of time-variable rates of change, which will allow to derive trend uncertainties for arbitrary intervals. Here we restrict ourselves on the formal uncertainties of trends.

The GRACE based Antarctic ice mass change are derived from spherical harmonic monthly solution series by ITSG-Grace2016 by TU Graz (Klinger et al., 2016; Mayer-Gürr et al., 2016) following a regional integration approach with tailored integration kernels that account for both the GRACE error structure and the information on different signal variance levels on the ice sheet and on the ocean (Horwath and Groh, 2016). The GRACE derived mass change time series at monthly intervals are provided for the basin-averaged Antarctic Ice Sheet along with the uncertainty estimates the methodology for which is described in the Antarctic_Ice_Sheet_cci Comprehensive Error Characterisation Report (Nagler et al., 2016), updated under https://data1.geo.tu-dresden.de/ais_gmb/source/ST-UL-ESA-AISCCI-CECR-Draft_GMB.pdf

The two AIS mass change time series are compared with two other external products: (1) AIS time series from the IMBIE-2 project over 1993-2015 (Shepherd et al., 2018) and (2) AIS mass change time series from WCRP (2018) over 2005-2015. The IMBIE-2 provides reconciled estimates of ice sheet mass change data using satellite altimetry, gravimetry and the Input-Output Method (IOM, Shepherd et al., 2018). The data used here provides cumulative AIS sea level contribution (equivalent sea level in mm) and its corresponding uncertainty is available at monthly resolution.

The datasets used in WCRP (2018) is the mean of Antarctica mass balance time series generated from GRACE based products and mass balance time series generated from IOM (update of Rignot et al., 2011) based product and is available at annual time resolution over 2005-2015. More information on each GRACE based product used can be found in WCRP (2018).

Figure 3.1a displays the SLBC_cci v1 altimetry based AIS sea level contribution (in mm) time series superimposed with the IMBIE 2 AIS sea level time series along with their respective uncertainty estimates. Over the 1993-2015 time period, the trend of altimetry-based SLBC_cci v1 Antarctica contribution is 0.17±0.03 mm/yr. The quoted error is the formal error based on the least-squares fit that accounts for the data uncertainties. The IMBIE-2 based trend estimate is 0.26 ±0.05 mm/yr.

Figure 3.1b displays the comparison of SLBC_cci v1 altimetry based and GRACE based AIS sea level time series with those of IMBIE-2, WCRP (2018). In terms of trend estimates over 2005-2015, the altimetry and GRACE based SLBC_cci v1 AIS contribution accounts to 0.39 ± 0.02 mm/yr and 0.32 ± 0.1 mm/yr respectively whereas the WCRP (2018) trend estimate is 0.45 ± 0.06 mm/yr and that of IMBIE 2 is 0.48 ± 0.04 mm/yr. Table 3.1 summarizes the trend estimates for each of components over three time periods: 1993-2015, 2003-2015 and 2005-2015.

a)

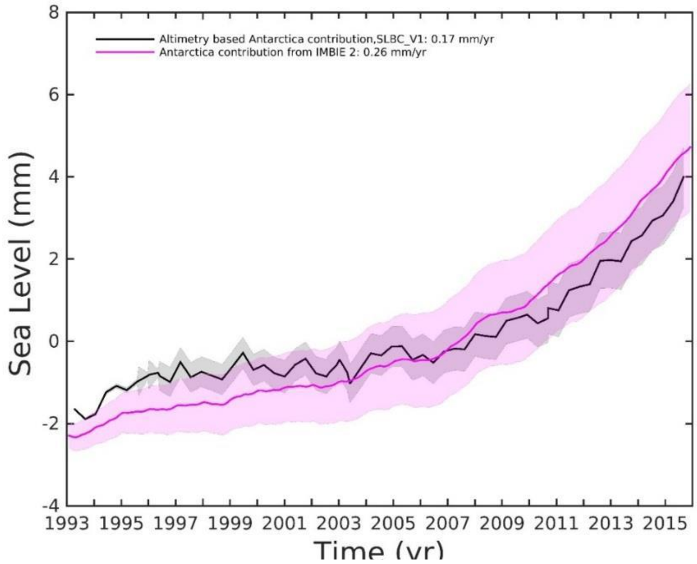

b)

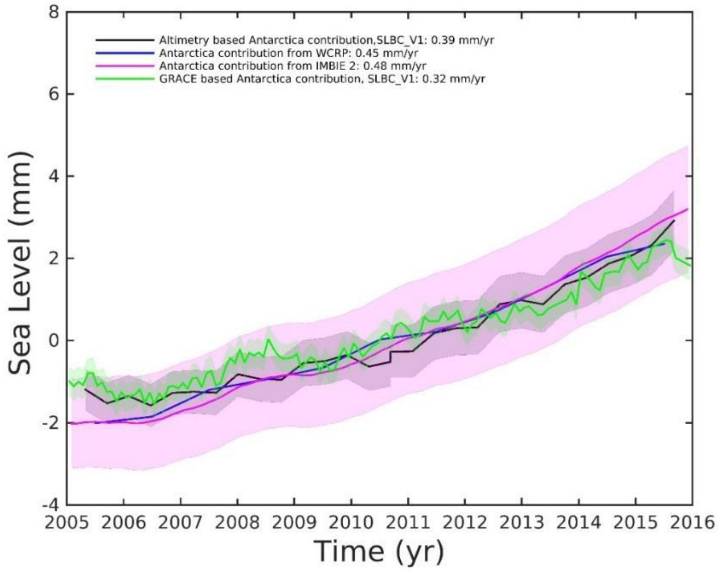

Figure 3.1: AIS sea level contribution (a) from SLBC_cci altimetry based (black) and IMBIE 2 (magenta) products over 1993-2015, and (b) from SLBC_cci altimetry based (black), WCRP (2018) (blue), IMBIE 2 (magenta,) and GRACE based (green) products over 2005-2015.

Table 3.1: Comparison of trend values over three time periods of the sea level components

Trend (mm/yr)	Antarctica Ice Sheet				Greenland Ice Sheet		
	SLBC_cci v1				SLBC_cci v1		WCRP (2018) / Bamber et al. (2018)
	Altimetry based	GRACE based	IMBIE 2	WCRP (2018)	Radar altime-try based	DTU GRACE based	
1993-2015	0.17 ± 0.03	~	0.26 ± 0.05	~	0,43	~	0.51±0.15
2003-2015	0.32 ± 0.02	0.28 ± 0.1	0.43 ± 0.04	~	0,68	0.78±0.025	0.79±0.03
2005-2015	0.4 ± 0.02	0.32 ± 0.1	0.48 ± 0.04	0.45±0.06	0,74	0.81±0.025	0.82±0.03

Trend (mm/yr)	Glaciers		TWS		
			SLBC_cci v1		Ensemble Mean GRACE (LEGOS)
	SLBC_cci v1	WCRP (2018)	Ensemble Mean TWS	ITSG GRACE	
1993-2015	0.6	0.65±0.05	0.25		
2003-2015	0.68		0.28		
2005-2015	0.7	0.77±0.18	0.3	0.37	0.06

Trend (mm/yr)		Steric			
	SLBC_cci v1	SLBC_cci v1.2	Dieng et al., 2017	WCRP (2018)	CMEMS
1993-2015	1.53		1.23	1.31	1.52
2003-2015		1.16	1.23	1.11	1.45
2005-2015	1.54		1.22	1.31	1.39

(b) Greenland Ice Sheet (GIS)

The SLBC_cci v1 database provides three different GIS mass change time series: (1) GIS mass change from lidar altimetry, (2) GIS mass change from radar altimetry and (3) GIS mass change from GRACE. However, the temporal coverage of lidar altimetry-based GIS mass change time series is only between 2003 and 2009 and is provided as 5-year mass change trend only and is therefore not used here. The radar-based GIS time series is the annual mean mass loss for GIS over 1992-2017. The data are calibrated using the 2003-2009 data from ICESat laser altimetry and snow/firn modelling to both account for firn changes and radar penetration. More information on this product is available in the Product Description Document D2.3.2. The uncertainty is provided in the data product as the standard deviation of the elevation change converted into mass as ice densities.

The GRACE based SLBC_cci v1 GIS mass change data is the time series of the mass change data based on the CSR RL06 spherical harmonics-based GRACE release. The method used for the inference of GIS mass change is an inversion approach as in Barletta et al. (2013). The time series is available at a monthly temporal resolution and covers the period 2003-2016. The GRACE based v1 GIS mass change time series is not corrected for GIA. Nevertheless, in our study, we apply the GIA contribution for Greenland mentioned to be -5.4 Gt/yr in the D2.3.2 Document (Page 82) which is based on A et al., 2013 ICE5g-VM2 model.

For comparison with external data, we use the GIS mass change data from WCRP (2018). Over the GRACE time starting from 2003, the WCRP GIS time series is an average of various GRACE based products as described in WCRP (2018) while prior to 2003, the time series between 1993 and 2002 is based on the IOM from van den Broeke et al. (2016). The WCRP (2018) time series is available at an annual time resolution. The error for each year has been calculated as the mean of all stated 1 sigma errors divided by $\sqrt{N}$ where N is the number of datasets available for that year, assuming that the errors are uncorrelated.

Figure 3.2a displays the SLBC_cci v1 radar based GIS contribution in terms of SLE (mm) and GIS sea level contribution from WCRP (2018) (and same as in Bamber et al., 2018) over 1993-2015 while Figure 3.2b displays the SLBC_cci v1 radar, GRACE base, and WCRP (2018)/Bamber et al. (2018) GIS contribution in terms of sea level over 2005-2015. Over the altimetry era of 1993-2015, the SLBC_cci v1 radar altimetry based GIS contribution in terms of trend is 0.41 mm/yr while that from WCRP (2018)/Bamber et al. (2018) is 0.51±0.15 mm/yr. Over the GRACE period of 2005-2015, radar altimetry based GIS sea level trend contribution is 0.74 mm/yr, GRACE based 0.81 ± 0.025 mm/yr and WCRP (2018)/Bamber et al. (2018) accounts to 0.82 ± 0.03 mm/yr. Refer to Table 3.1 for summarized trend values. While the trend estimates of the various processing methods over both the time periods remain very close to each other (with differences only in the range of 0.1 mm/yr), from the figures we can observe that the range of uncertainty in each of these data sets are different from each other and in cases such as the radar based SLBC_cci v1 and WCRP (2018) GIS data, the uncertainty range is very high. The Product Description Document mentions that the radar altimetry based SLBC_cci v1 GIS data indeed slightly overestimate the combined error of the five error sources (D2.3.2, page 82). Note that Table 3.1 does not quote uncertainties for radar-altimetry-based GIS trends. While the time series are provided with uncertainties of cumulated changes since 1993, a different assessment is needed to derive uncertainties for trends over sub-intervals such as 2003-2015 or 2005-2015. Such an assessment is being done in the final version 2 phase of SLBC_cci.

a)

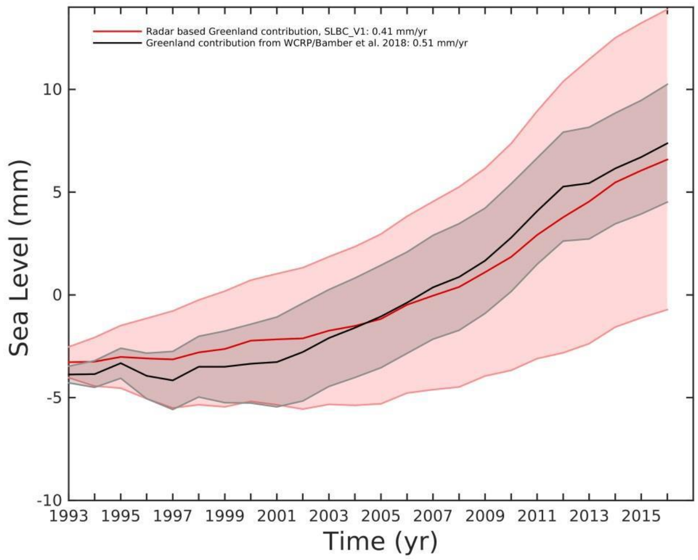

b)

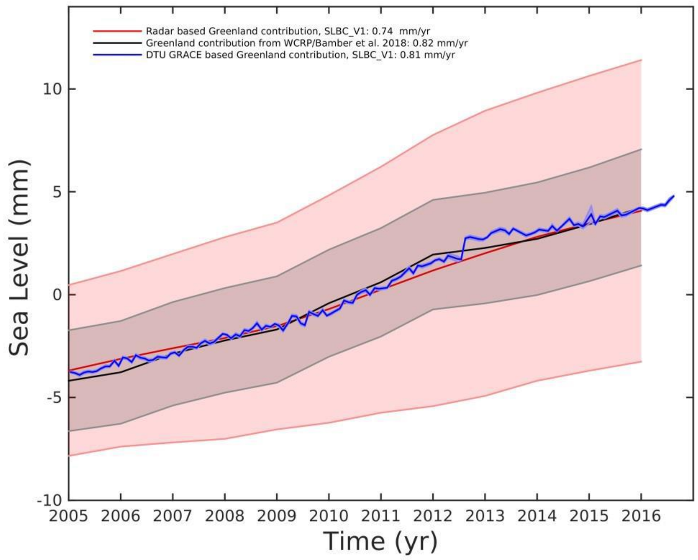

Figure 3.2: GIS sea level contribution from (a) SLBC_cci radar altimetry based (red) and WCRP (2018)/Bamber et al. (2018) (black) products over 1993-2015, and (b) from SLBC_cci radar altimetry based (red), SLBC_cci v1 DTU GRACE based (blue) and WCRP (2018)/ Bamber et al. (2018) (black), products over 2005-2015.

3.1.2.1 Glaciers

The SLBC_cci v1 glacier mass balance data is based on the glacier evolution model that requires several input variables such as global glacier outlines, atmospheric boundary conditions, measured mass balances etc. (Marzeion et al., 2012). The SLBC_cci v1 glacier evolution model has used several different data sets for each of these input parameters (refer to D2.3.2, page

57) and has been calibrated and validated using World Glacier Monitoring Service (WGMS, 2016) observational glacier mass balance. The SLBC_cci v1 data base provides two main variables: (1) Gridded glacier mass change in terms of Gt. The global values are obtained by summing over the global grid. (2) Uncertainties of glacier mass change, also expressed in Gt as global gridded data. Global values of the uncertainty are obtained by taking the square root of the sum of the squares of these uncertainties over the region of interest (globally in this case). To convert the given uncertainties to standard uncertainties, the numbers are divided by 1.645 (as mentioned in D2.3.2, page 60). Both the variables are provided at monthly temporal resolution over 1979-2016. Uncertainties provided with v1 glacier data and plotted in Figure 3.3 are subject to an error, which will be fixed for v2. Therefore, glacier trends are quoted without uncertainties in Table 3.1 and in the subsequent analyses.

The external source of glacier mass change data used here for comparison is the data from WCRP (2018). This data comprises of an ensemble mean of glacier mass change from five estimates: update of Gardner et al., 2013, update of Marzeion et al. 2012, update of Cogley 2009, update of Leclercq et al., 2011 and average of GRACE based estimates of Marzeion et al., 2017. Over 2005-2015, WCRP (2018) provides annual glacier mass change from the ensemble mean whereas as over 1993-2015, only the trend estimate is provided.

Figure 3.3 displays the SLBC_cci v1 glacier contribution to sea level (in terms of mm) over 1993-2015 to which the WCRP (2018) glacier contribution sea level time series is superimposed over 2005-2015. Over the 1993-2015 time period, the SLBC_cci based trend amounts to 0.6 mm/yr whereas that of WCRP (2018) is 0.65 ± 0.05 mm/yr. Over 2005-2015, the WCRP (2018) trend value is 0.77 ± 0.18 mm/yr (0.7 mm for . SLBC_cci v1).

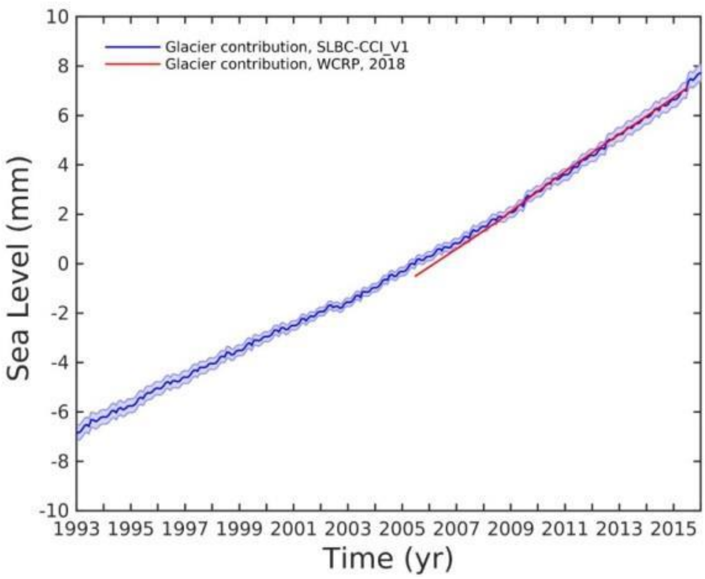

Figure 3.3: Glacier mass change contribution to sea level (in terms of e.s.l., mm) from SLBC_cci v1 (blue) and WCRP (2018) (red) products 1993-2015 and 2005-2015 respectively.

3.1.2.2 Total land Water Storage

The SLBC_cci v1 provides global averaged and gridded time series of total land water storage (TWS) based on the WaterGAP 2.2c global hydrological model standard. Two variants of WaterGAP 2.2c corresponding to two irrigation scenarios (70% deficit scenario and 100% or optimal irrigation scenario) are provided, each of which uses three climate forcings: daily WFDEI using GPCC precipitation, WFDEI using CRU TS 3.23 precipitation and CRU TS 4.00 forcing. Thereby, a total of six datasets are available. The time series are available at monthly time resolution over 1993-2015.

Figure 3.4 displays the TWS contribution to sea level (in terms of e.s.l. mm) of all the six datasets between 1993 and 2015. We may note that WFDEI-GPCC time series end in 2013. This is due to unavailability of GPCC precipitation data beyond 2013. Therefore, in this study we have considered only 4 data sets (WFDEI-CRU and CRU TWS data under two irrigation scenarios). Table 3.2 displays the TWS trend values of the four datasets over three different time periods of study.

From Figure 3.4, we can observe that in terms of interannual variability the TWS time series for both 70% irrigation deficit and 100 % optimal scenario do not display major differences. In terms of trend estimates, over the three periods of study, trends from 100% optimal scenario for CRU TS 4.0 and WFDEI-CRU are slightly higher than those at 70 % irrigation scenario. Furthermore since model based uncertainty estimates are not yet available, we estimated TWS uncertainty at each time step by estimating the Root Mean Square (RMS) of the dispersion of each time series from the mean.

Table 3.2: TWS trend estimates for SLBC_cci v1 products for two different irrigation scenarios and two different forcings.

Trend in mm/yr	**CRU TS 4.0**		**WFDEI-CRU**	
	70% deficit	100% optimal	70% deficit	100% optimal
1993-2015	0.26	0.37	0.24	0.36
2003-2015	0.24	0.34	0.31	0.43
2005-2015	0.33	0.44	0.4	0.51

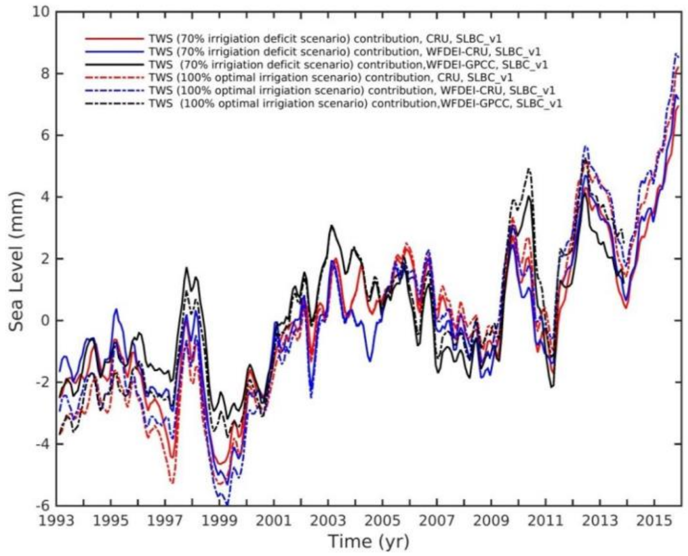

Figure 3.4: TWS contribution to sea level (in terms of e.s.l., mm) from SLBC_cci v1 for two irrigation scenarios, (1) 70% irrigation deficit as solid lines and (2) 100% optimal irrigation scenario as dashed lines over 1993-2015. CRU TS 4.00 in red, WFDEI-CRU in blue and WFDEI-GPCC in black.

As external sources of TWS time series for comparison with SLBC_cci v1 TWS time series based on hydrological models, we used two products: (1) An ensemble mean of GRACE mascon based TWS time series from CSR, JPL and GSFC over 2005-2015. This TWS time series was estimated at LEGOS by summing up the land water storage contribution from 343 major hydrological basins in the world obtained from Global Run-off Data Center (GRDC) shapefiles. Using GRDC shapefiles instead of globally averaging land mass GRACE data makes ensures that only the hydrological basins are accounted for in the TWS estimation and thereby glaciers are not considered. (2) An estimate based on averaging GRACE data over the whole continental area, as provided by TU Dresden. This product uses the ITSG Grace2016 data. Since the ITSG Grace land water time series also include glacier contribution that accounts to 0.7 mm/yr over 2005-2015, we removed it from the time series over 2005-2015.

Figure 3.5 displays the TWS time series from the three above mentioned datasets over 2005-2015. We can observe that the interannual variability is well reproduced in hydrological model based TWS and the two GRACE based TWS time series. There is a very good agreement between the WGHM v1 product and the ITSG GRACE TWS, both in terms of trend (0.42 mm/yr and 0.37 mm/yr respectively, Table 3.3) and interannual variability. The GRACE mascon-based TWS over the 346 basins has a very small trend, of 0.06 mm/yr only. We are currently trying to understand the source of the trend discrepancy seen between the two SLBC_cci v1 products and the ensemble mean GRACE mascon product.

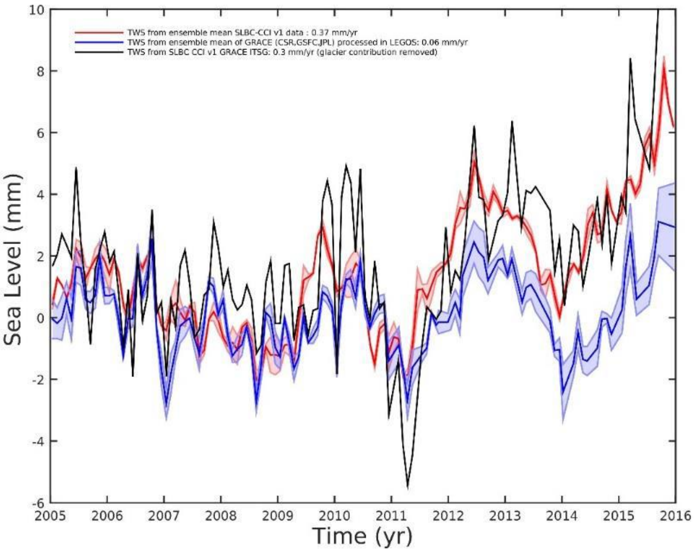

Figure 3.5: TWS contribution to sea level (in terms of e.s.l.,, mm) from ensemble mean SLBC_cci v1 hydrological models (in red), ensemble mean GRACE mascons from LEGOS (in blue) and SLBC_cci v1 ITSG GRACE (in black) over 2005-2015.

Table 3.3: TWS trend estimates from SLBC_cci v1 hydrological model, SLBC_cci v1 ITSG GRACE and Ensemble GRACE mascon from LEGOS over 1993-2015, 2005-2015, and 2005-2011.

Trend in mm/yr	**SLBC_cci v1 data**		**LEGOS**
	Ensemble mean of WFDEI-CRU and CRU TS 4.0	ITSG GRACE	Ensemble GRACE mascon (CSR, JPL, GSFC)
1993-2015	0.31		
2005-2015	0.42	0.37	0.06

3.1.3 Ocean mass component from GRACE

Ocean mass products derived from the GRACE satellite mission were also used to analyze the sea level budget. The SLBC_cci v1 provides one main product, namely ITSG Grace2016 (Klinger et al., 2016, Mayer-Gürr et al., 2016) based on spherical harmonics solution. In addition, several other supplementary v1 products such spherical harmonics based CSR, JPL, GFZ Release 5 GRACE data, GSFC mascon based GRACE (Luthcke et al., 2013) and Chambers based GRACE ocean mass data (Johnson and Chambers, 2013, Chambers and Bonin, 2012).

The SLBC_cci v1 main product (ITSG) and other SH based supplementary products provided here have undergone various processing and corrections (refer to D2.3.2, pages 38-43). Furthermore, the spherical harmonics-based solutions have been provided with two types of GIA corrections: (1) GIA removal based on A et al. (2013), (2) GIA removal based on Caron et al. (2018). Ocean mass data without GIA correction is also provided. However, this data is not considered here.

Here we consider the globally averaged ocean mass change data from GRACE provided at a monthly time resolution between mid-2002 and end of 2016. The globally averaged ocean mass datasets also provide uncertainty values at monthly time steps estimated based on different sources of errors such as GRACE errors, leakage errors, GIA uncertainty etc. Two types of uncertainty are provided: (1) uncertainty due to noise, (2) systematic errors of the linear trend. As mentioned in the D2.3.2 document (page 52), the uncertainties at each time step are combined in the form of

$$\sigma_{total}^2(t) = \sigma_{noise}^2 + \left(\sigma_{trend} \cdot (t - t_0)\right)^2$$

for time-series of mass change $\Delta M(t)$-$\Delta M(t_o)$ with respect to a reference time t_o.

Figure 3.6 displays the GRACE based ocean mass time series over 2003-2015 from various processing groups with the two different GIA corrections applied. Their corresponding trend estimates over the same period of study are indicated in Table 3.4. The trend estimates of the spherical harmonics-based GRACE ocean mass from ITSG (SLBC_cci main product) and from CSR, JPL, GFZ account to the same value over 2003-2015. Differences in the order of 0.2 mm/yr arise between the two GIA correction methods considered, with Caron et al. (2018) GIA corrected ocean mass exhibiting higher range of trend than the A et al. (2013) GIA corrected GRACE ocean mass time series. Comparison with GSFC Mascon based ocean mass and Chambers spherical harmonics-based ocean mass show that the ITSG, CSR, JPL and GFZ ocean mass time series processed as part of SLBC_cci v1 are slightly lower than the ocean mass contribution when compared to other products in the range of 0.3-0.4 mm/yr for A et al. (2013) GIA correction and in the range of 0.2-0.3 mm/yr for Caron et al. (2018) GIA correction.

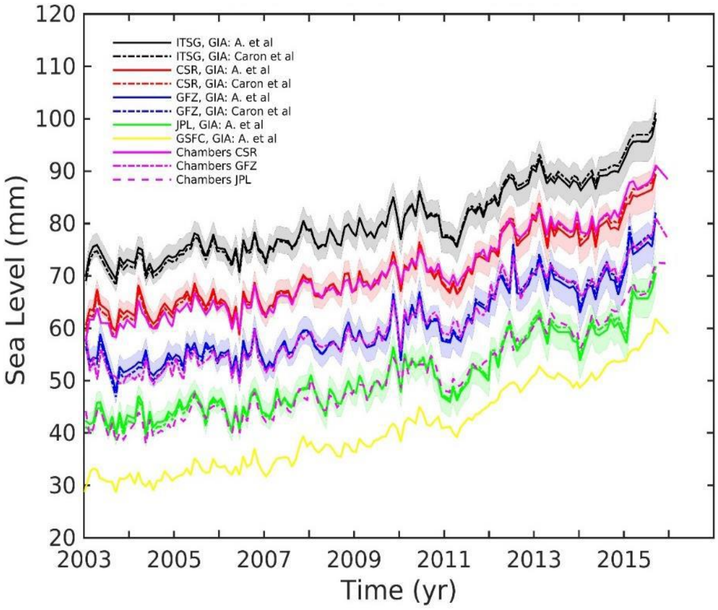

Figure 3.6: GRACE based ocean mass contribution in mm from various processing groups with two different GIA corrections over 2005-2015. The main SLBC_cci v1 product is ITSG (in black) while all others shown correspond to supplementary GRACE products.

Table 3.4: Trend estimates of GRACE based ocean mass time series over 2003-2015.

Trend (mm/yr)	**2003-2015**		
	Product	GIA correction	
		A. et al. (2013)	Caron et al. (2018)
SLBC_cci v1 Main product	ITSG SH	1.69 ± 0.24	1.89± 0.24
SLBC_cci v1 Suppl. products	CSR SH	1.66 ± 0.24	1.86± 0.24
	GFZ SH	1.69± 0.24	1.89± 0.24
	JPL SH	1.71± 0.24	1.91± 0.24
	GSFC Mascon	2.14	NA
	Chambers et al. CSR SH	2.05	NA

As an external source of comparison we also compared the SLBC_cci v1 GRACE ocean mass main product with the ensemble mean GRACE ocean mass time series from WCRP (2018). This time series is an ensemble mean of GRACE ocean mass time series from several processing groups such as updated CSR forward modelling from Chen et al. (2013), Chambers ocean mass products, and mascon-based CSR, JPL and GSFC products. This is available at annual time resolution over 2005-2016. They all have been corrected for GIA using A. et al. (2013) methodology.

Figure 3.7 displays the two GIA corrected SLBC_cci v1 ITSG time series superimposed to ensemble mean GRACE ocean mass time series from WCRP (2018) over 2005-2015. The ocean mass trend from WCRP (2018) is 2.2±0.19 mm/yr, whereas from those of ITSG are 1.86±0.24 mm/yr and 2.05±0.24 mm/yr for A et al. (2013) and Caron et al. (2018) GIA corrections, respectively. As with other supplementary GRACE ocean mass products already compared, the SLBC_cci v1 main ocean mass time series time series trend estimate over 2005-2015 still remains slightly lower.

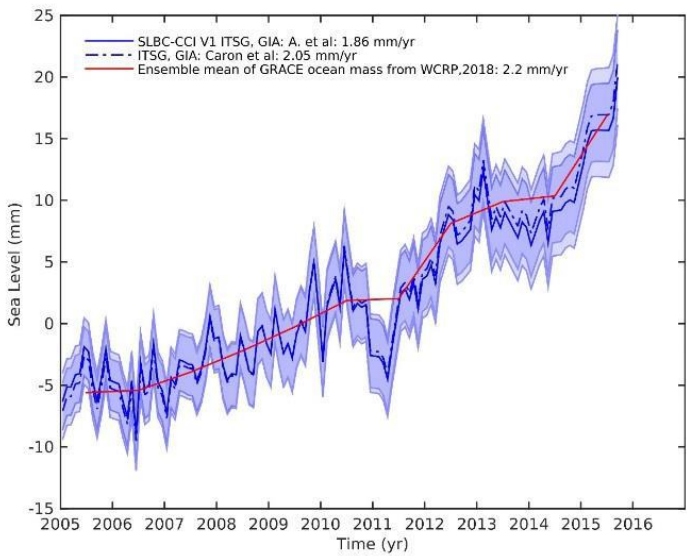

Figure 3.7: SLBC_cci v1 ITSG GRACE ocean mass time series corrected for A et al. (2013) and Caron et al. (2018) GIA in blue, and ensemble mean GRACE ocean mass time series from WCRP (2018) in red over 2005-2015.

3.1.4 Steric sea level component

The SLBC_cci v1 steric product consists of globally averaged and gridded 5°x5° time series of monthly mean Steric Sea Level Anomaly (SSLA) based on XBT and XCTD and ARGO profiles from the UK Met Office EN4.2.1 archive. The profiles are processed onto common vertical levels up to a depth of 2000m using the box averaging method developed by von Schuckmann and Le Traon (2011). The EN4.2.1 climatology for 1993-2015 is used. The gridded data as well as the derived global mean steric time series are provided with uncertainties estimated using the method developed at UoR taking into account the uncertainty in the original temperature (T) and salinity (S) observations and in the climatological (T,S) data, the effects of error correlation, and the spatial and temporal distribution of the sparse profile data within a cell.

As external sources of comparison we used the thermosteric sea level time series from WCRP (2018) and the ensemble mean steric sea level time series from Dieng et al. (2017) over 1993-2015. The thermosteric time series estimated until the depth of 2000 m from WCRP (2018) is an ensemble mean from 11 different processing groups that have used XBTs and CTDs during the pre-Argo era (i.e. from 1993 until 2003/2005), followed by Argo floats data until 2015. Detailed explanation on the data sets used and the processing can be found in WCRP (2018). The ensemble mean steric time series from Dieng et al. (2017) comprises the following three data sets for the period 1993-2004: the updated versions of Ishii and Kimoto (2009), NOAA data set (Levitus et al., 2012) and EN4 data set (Good et al., 2013). Over the recent years, these data sets integrate Argo data from IPRC, JAMSTEC and SCRIPPS.

Figure 3.8a and Figure 3.8b display the SLBC_cci v1 steric sea level time series superimposed to ensemble mean steric from Dieng et al. (2017) and thermosteric from WCRP (2018) over 1993-2015 and 2005-2015 respectively. The trend values among the three datasets vary only by a maximum of 0.2 mm/yr over the two-time periods (see Table 3.1 for trend estimates). However, in terms of interannual variability, the SLBC_cci v1 steric time series shows large discrepancies before the Argo era, i.e. between 1993 and 2005. To better highlight the discrepancy, we also estimated a *'residual steric'* time series computed from (1) the difference between the observed global mean sea level (GMSL) and sum of mass components (v1 products delivered by the partners), on which is superimposed the SLBC_cci v1 steric data, and (2) *'residual steric'* time series computed from the difference between the observed GMSL and sum of mass components (v1 products delivered by the partners), on which is superimposed the ensemble mean steric data used in Dieng et al. (2017) as displayed in Figure 3.9a. The corresponding differences between the *'residual steric'* from the budget and each steric time series are shown in Figure 3.9b. The two figures show the huge discrepancy before the Argo era very well. Data from Dieng et al. (2017) is used in the residual estimation and not the data WCRP (2018) as the latter only provides annual mean time series.

The RMS have been estimated from the difference time series shown in Figure 3.9b. These are also reported in Table 3.5. We note higher RMS when the SLBC_cci v1 steric data is used whatever time span considered. In particular, prior to Argo, the residuals are more than twice as large as the ensemble mean case.

On personal communication with the SLBC_cci v1 steric partner, the SLBC_cci v1 steric data has been found to have certain bugs that have now been fixed and a newer release from the SLBC_cci partner v1.2 of steric sea level time series is now available. This has now been used in the budget assessment along with previously used steric sea level data from Dieng et al. (2017) and thermosteric sea level data from the Copernicus Project, CMEMS provided by Dr. von Schuckmann as v1 steric replacement.

Table 3.5: RMS estimated from the difference time series shown in Figure 3.9b

RMS in mm	1993-2015 (Full)	1993-2004 (Pre-Argo)	2005-2015 (Argo)
Residual steric (from the budget) minus SLBC_cci v1 steric	4.6	5.8	2.8
Residual steric (from the budget) minus Ensemble Mean steric (Dieng et al., 2017)	2.2	2.4	2.0

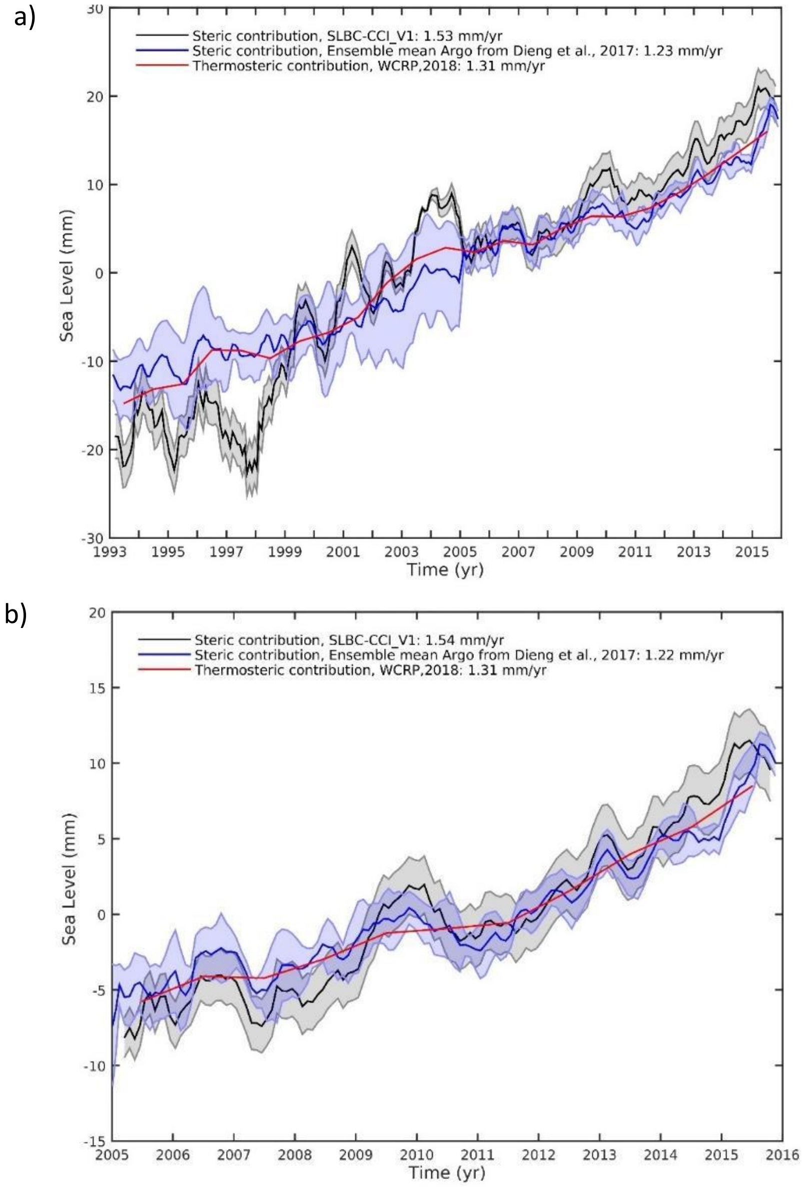

Figure 3.8: SLBC_cci v1 steric sea level time series superimposed to ensemble mean steric from Dieng et al. (2017) and thermosteric from WCRP (2018) over (a) 1993-2015 and (b) 2005-2015.

a)

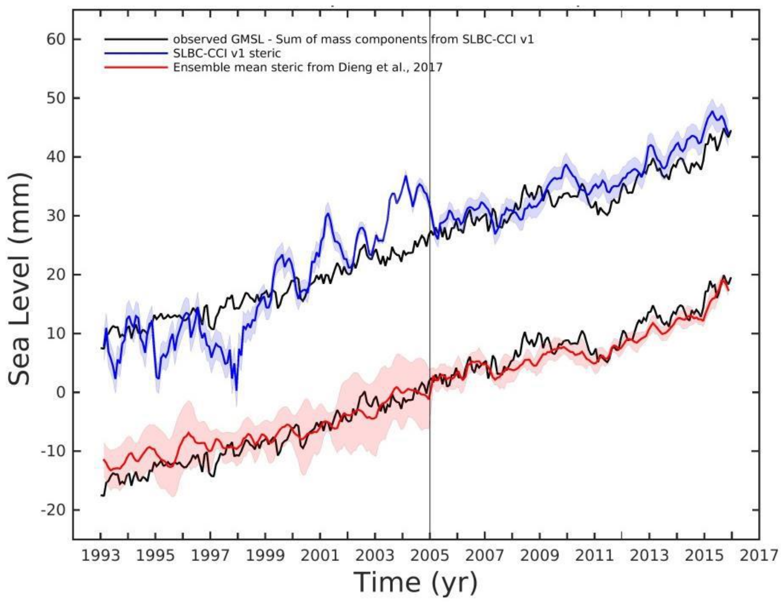

b)

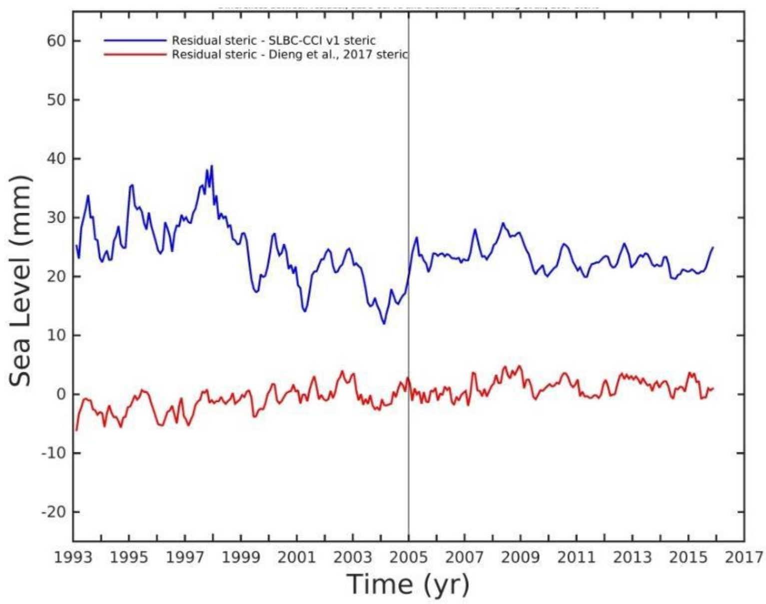

Figure 3.9: (a) Upper curves: 'residual steric' time series (black) computed from the difference between the observed GMSL and sum of mass components (v1 products delivered by the partners), on which is superimposed the v1 steric data (blue); Lower curves: black curve same as above, red curve: ensemble mean steric data used in Dieng et al. (2017). (b) Upper curve: Difference between the 'residual steric' time series based on the budget and the v1 steric data (blue). Lower curve: Difference between the 'residual steric' time series based on the budget and the ensemble mean used in Dieng et al. (2017) (red).

Thermosteric sea level component from CMEMS

CMEMS provides two sets of globally averaged (60°N-60°S) thermosteric sea level time series over 1993-2017 and over 2005-2017. The thermosteric time series that cover the entire altimetry era is until a depth of 700 m while the time series between 2005 and 2017 extend until a depth of 2000 m. These time series are an ensemble mean of GLORYS2V4, C-GLORS, ORAS5, ARMOR3D reanalysis data. More information on the product can be found at http://marine.copernicus.eu. An ensemble spread of the globally averaged thermosteric sea level time series (cf. Dieng et al. 2017) is also available for each product.

Figure 3.10a displays the comparison of CMEMS thermosteric sea level (0-700 m) over the altimetry era 1993-2015 with steric sea level time series from Dieng et al. (2017) and thermosteric sea level from WCRP (2018) while Figure 3.10b displays CMEMS thermosteric (0-2000 m with deep ocean contribution included) comparison with the same over 2005-2015. Over 1993-2015, CMEMS thermosteric sea level trend accounts to 1.52±0.09 mm/yr, whereas those of Dieng et al. (2017) and WCRP (2018) are 1.23 ± 0.12 mm/yr and 1.31 mm/yr, respectively. Considering that the CMEMS thermosteric covers only until a depth of 700 m and also the fact that the trend value being at the higher end seems like a discrepancy, henceforth has been decided not to use this dataset over the altimetry era for budget analysis. Over the 2005-2015 time period, the thermosteric sea level trend from CMEMS (until a depth of 2000m) accounts to 1.39±0.1 mm/yr and is in the range of steric and thermosteric sea level trend values from Dieng et al. (2017) and WCRP (2018) respectively.

SLBC CCI v1.2 steric sea level component from University of Reading

The SLBC_cci v1.2 globally averaged steric sea level anomaly is similar to that of v1 product i.e. globally averaged from a gridded 5°x5° time series of monthly mean Steric Sea Level Anomaly (SSLA). The v1.2 time series is however based only on Argo profiles and henceforth is available from 2002. Furthermore, the climatology is estimated using EN4.2.1 data over 2006-2015.

Figure 3.11a and Figure 3.11b display comparisons of SLBC_cci v1.2 steric sea level time series with those of Dieng et al., 2017, thermosteric from WCRP, 2018 and CMEMS over 2003-2015. The SLBC_cci v1.2 steric time series perform much better than the v1 time series in terms of both interannual variability and trend (Table 3.1) when compared with other products.

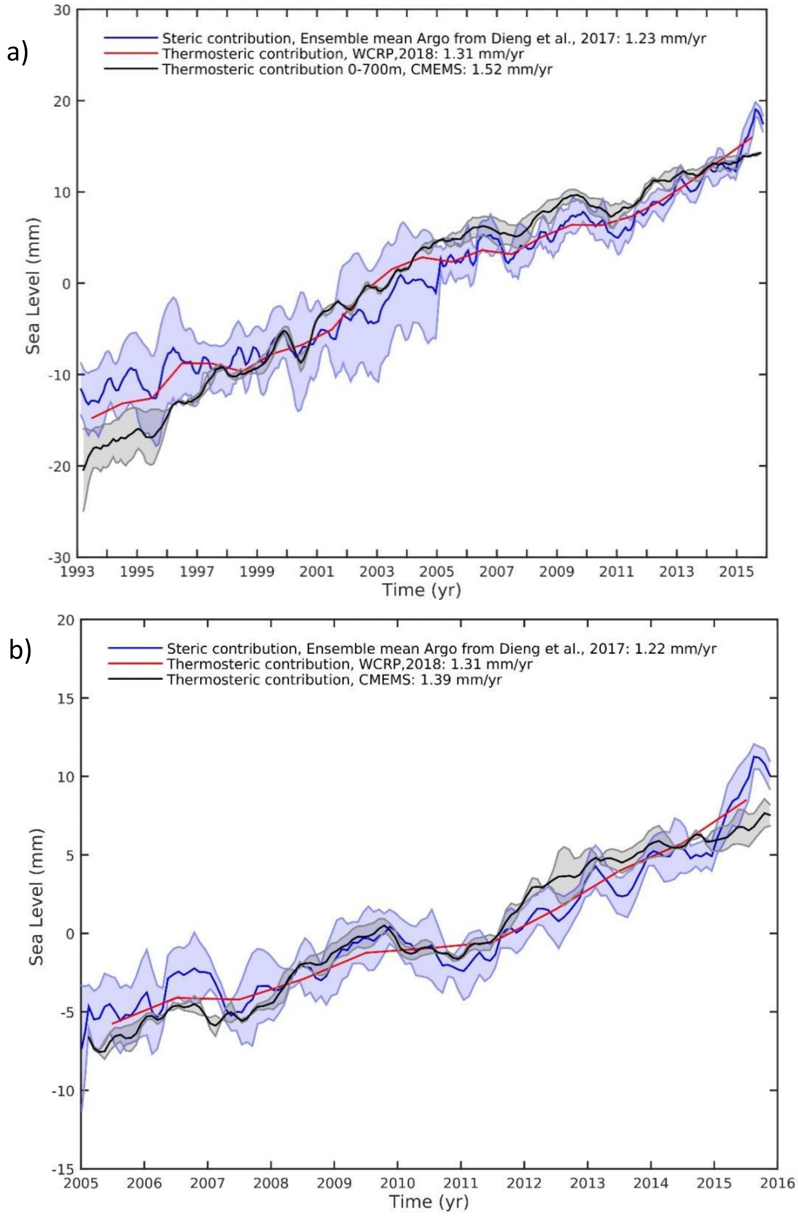

Figure 3.10: CMEMS thermosteric sea level time series superimposed to ensemble mean steric from Dieng et al. (2017) and thermosteric from WCRP (2018) over (a) 1993-2015 and (b) 2005-2015.

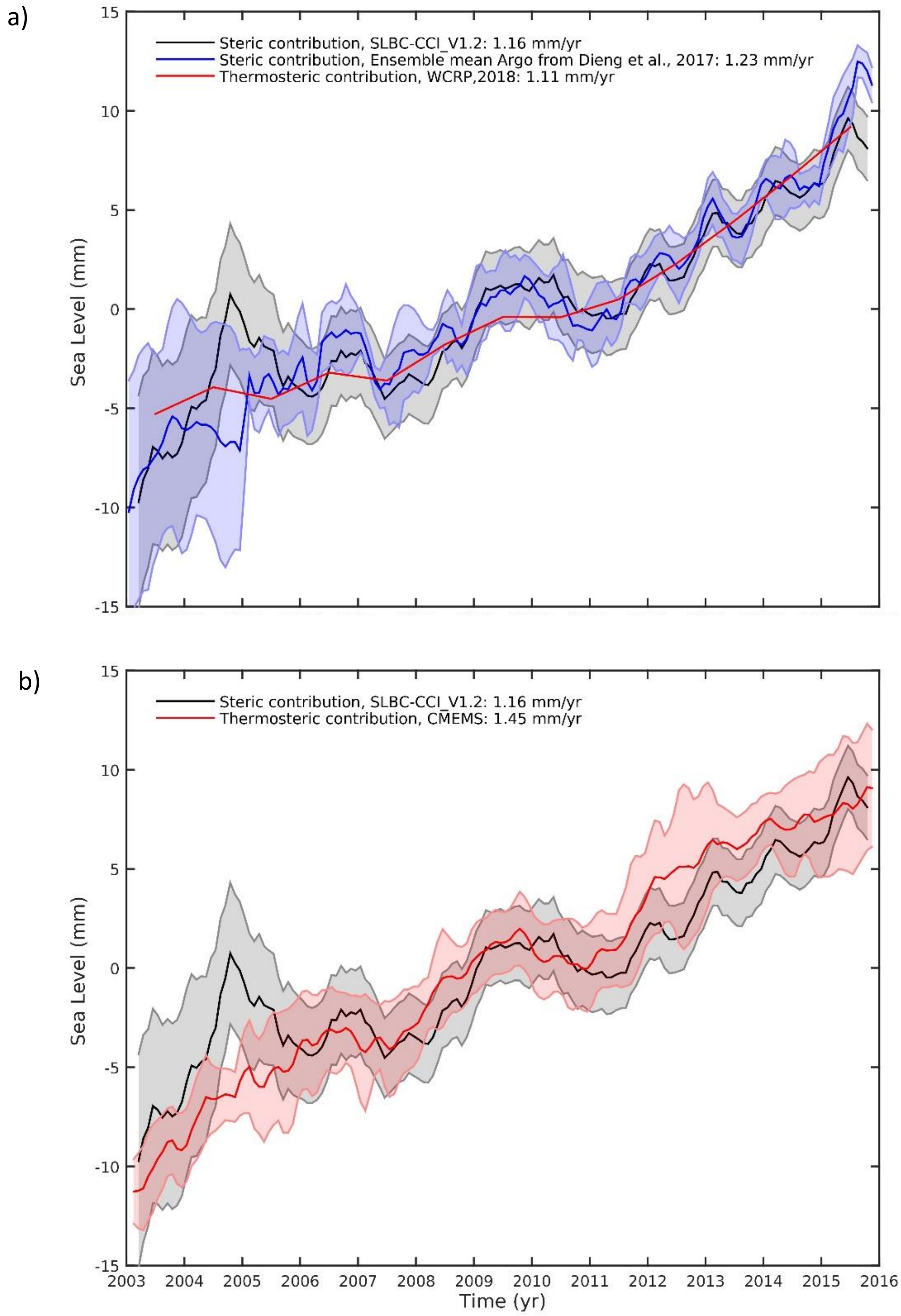

Figure 3.11: Comparison of SLBC CCI v1.2 steric sea level time series with (a) steric from Dieng et al., 2017 and thermosteric from WCRP, 2018; (b) thermosteric from CMEMS over 2003-2015.

3.2 Budget assessment

The sea level budget closure assessment was performed using two approaches: (1) comparison of observed sea level with sum of individual components from SLBC_cci v1, and (2) with GRACE-based ocean mass for the mass components. Two-time periods were considered:

Period 1 (P(1)): the entire altimetry era, 1993-2015, where the sea level budget closure was investigated by comparing observed rate of sea level rise with the sum of contributions estimated independently.

Period 2 (P(2)): over the Argo/GRACE era, 2003-2015, where the sea level budget closure was investigated by comparing observed rate of sea level first with the sum of contributions as in P(1) and then with the sum of steric and GRACE based ocean mass.

3.2.1 Period P(1): the altimetry era (1993-2015)

The global mean sea level budget was estimated by comparing the GMSL observed by satellite altimetry with the sum of the SLBC_cci v1 components except for the steric sea level component over 1993-2015, where steric data from Dieng et al. (2017) was used. In the case of satellite altimetry based GMSL time series, we used the CCI based Ablain et al. (2017) GMSL time series (sc. Section 3.1.1).

Figure 3.12 displays the global mean sea level budget estimated as the sum of individual SLBC_cci v1 components superimposed to the altimetry-based GMSL. Individual components are also displayed. The global mean sea level trend (Table 3.6) obtained as the sum of individual SLBC_cci v1 components over 1993-2015 accounts to 2.74 mm/yr, whereas observed GMSL trend value accounts to 2.92±0.3 mm/yr leaving a residual of 0.18 mm/yr as seen in the residual time series (observed GMSL minus sum of components). In terms of interannual variability, the GMSL obtained from the sum of components corresponds well with observed altimetry-based CCI GMSL, except in the beginning years. This is expected, as the TOPEX A drift correction between 1993 and 1998 is not yet precise and the steric component based on XBT data suffers from sparse coverage both geographically and at depth (below 700 m). The RMS of the residual time series over 1993-2015 amounts to 2.9 mm.

Table 3.6: Observed GMSL trend compared with sum of components trend over 1993-2015

Trend (mm/yr)	1993-2015
Observed CCI GMSL	**2.92 ± 0.3**
Steric, Dieng et al. (2017)	1.23 ± 0.12
Antarctic Ice Sheet	0.17± 0.03
Greenland Ice Sheet	0.43
Glacier	0.6
Total land Water Storage	0.31 ± 0.01
Sum of components	**2.74**
Residual	0.18
RMS (mm)	2.9

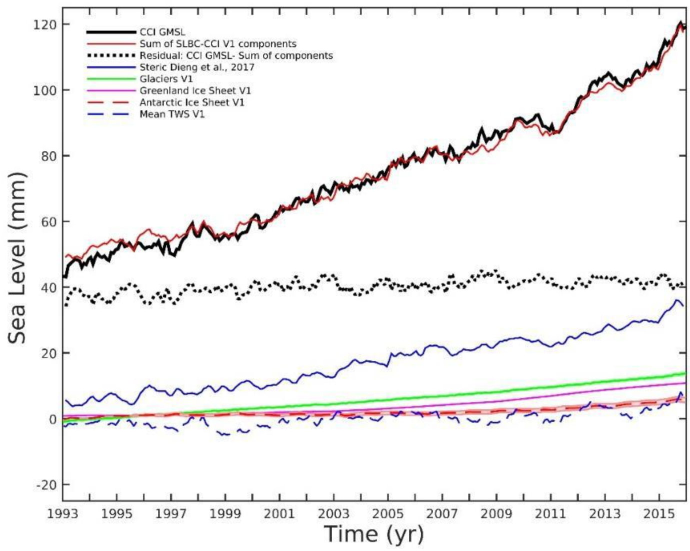

Figure 3.12: Observed CCI GMSL (black) superimposed with the GMSL estimated from the sum of SLBC_cci v1 sea level components (in red) over 1993-2015.The residual time series (i.e. CCI GMSL- sum of components) is shown as dotted black time series. The individual components, steric (in blue), glaciers (in green), Greenland (in magenta, altimetry-based), Antarctica (dashed red, altimetry-based) and TWS (dashed blue) are also displayed. Curves are arbitrarily shifted along the ordinate axis for better legibility. For example, the residual time series is shifted by 40 mm.

3.2.2 Period P(2): the ARGO/GRACE era (2003-2015)

For this time period, the sea level budget closure was investigated by comparing observed GMSL first with the sum of individual SLBC_cci v1 sea level components as in P(1) (explained in the previous section) and then with the sum of steric and GRACE based ocean mass. Table 3.7 summarizes the trend value of observed CCI GMSL and sum of each SLBC_cci v1 components contributing to sea level variations over 2003-2015. For the 2003-2015 period, the steric data from this project (steric v1.2) has been used. Sea level budget assessment over this time period was performed using two different sets of AIS and GIS data: (1) altimetry based, (2) GRACE based AIS and GIS contribution. In Table 3.7, the GRACE based contributions and henceforth the corresponding sea level budget are shown in *italic*. From the table, we can observe that the differences between altimetry based and GRACE based AIS/GIS contributions are not major with the sum of individual components adding up to 3.22 mm/yr and 3.25 mm/yr, respectively, thereby leaving a residual of 0.2mm/yr and lesser in both cases. Figure 3.12 displays the global mean sea level budget estimated as the sum of individual SLBC_cci v1 sea level components (in red) superimposed to the CCI observed altimetry based global mean sea level time series (in black) over 2003-2015 and its corresponding residual (dotted black line). The individual components are also displayed in the same figure. Altimetry based AIS and GIS time series are depicted in Figure 3.13 (GRACE based time series are also similar and henceforth not shown here).

Table 3.7: Observed CCI GMSL trend compared with sum of components trend over 2003-2015. GRACE based AIS and GIS contributions and their corresponding budget trend values are in blue.

Trend (mm/yr)	**2003-2015**
Observed CCI GMSL	**3.42 ± 0.3**
Steric v1.2	1.16 ± 0.2
Antarctic Ice Sheet: Altimetry based/ *GRACE based*	0.33/ *0.28 ±0.1*
Greenland Ice Sheet: Radar alti.based/ *GRACE based*	0.7/ *0.78 ± 0.025*
Glacier	0.7
Total land Water Storage	0.33 ± 0.07
Sum of components	**3.22/ *3.25***
Residual	0.2/ *0.17*

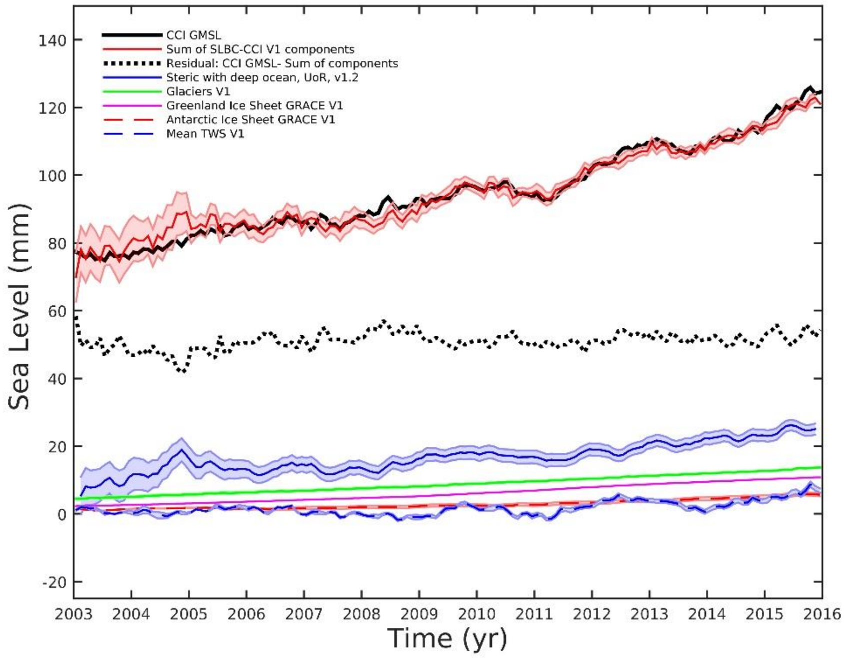

Figure 3.13: Same as in Figure 3.12 but over 2003-2015

Sea level budget using GRACE ocean mass

Over 2003-2015 time period corresponding to the Argo/GRACE era, the individual mass components (glaciers, AIS, GIS, TWS) can be replaced by ocean mass directly observed by GRACE. Therefore, over this time period the sea level budget was also performed using the main and supplementary SLBC_cci v1 GRACE ocean mass products. Figure 3.14 displays the observed CCI global mean sea level time series superimposed with the global mean sea level estimated as the sum of steric from SLBC_cci v1.2 and various GRACE ocean mass products (different colours corresponding to different GRACE product). Their corresponding residuals ($GMSL_{observed}$-$GMSL_{(steric+GRACE)}$) are also displayed as dotted lines in the same figure. Table 3.8 summarizes their corresponding trend values, residual trends and RMS. From the figure, we can see that between 2005 and 2010 the sum of steric and almost every GRACE product corresponds very well with the observed CCI GMSL, whereas from 2011, the dispersion between the observed CCI GMSL and the steric + GRACE increases. This is also evident from the residual time series where we observe evident dispersion from 2011 in all GRACE products. The discrepancy between observed CCI GMSL and steric+GRACE between 2003 and 2005 is mainly due to steric data as between 2003 and 2005, the Argo transition was not complete and hence lesser Argo floats data are available. In terms of residual trend, i.e. $GMSL_{observed}$-$GMSL_{(steric+GRACE)}$, residuals involving GSFC mascon based and Chambers based mean GRACE

Table 3.8: Observed CCI GMSL trend compared with steric + GRACE ocean mass over 2003-2015.

Trend (mm/yr)	2003-2015			
	ITSG A et al.,2013	**ITSG Caron et al., 2018**	**GSFC Mascon**	**Mean Chambers**
Obs.GMSL	3.32 ± 0.3	3.32 ± 0.3	3.35 ± 0.3	3.3 ± 0.3
Steric v1.2	1.12 ± 0.2	1.12 ± 0.2	1.12 ± 0.2	1.12 ± 0.2
GRACE	1.69 ± 0.24	1.89 ± 0.24	2.14	2.04 ± 0.15
Sum	2.81 ± 0.31	3.01 ± 0.31	3.26	3.16 ± 0.25
Residual	0.51 ± 0.43	0.31 ± 0.43	0.09	0.14 ± 0.4
RMS (mm)	3.34	2.96	2.5	2.6

data produce the least residuals, 0.09 mm/yr and 0.14 mm/yr respectively. In the case of ITSG GRACE, the SLBC_cci v1 main product, the residual obtained used GRACE data corrected for Caron et al. (2018) results in a lesser residual trend value than the A et al. (2013) GIA corrected GRACE. The steric + GRACE and the residual trend uncertainties are estimated as the root square sum (RSS) of the steric and GRACE uncertainties.

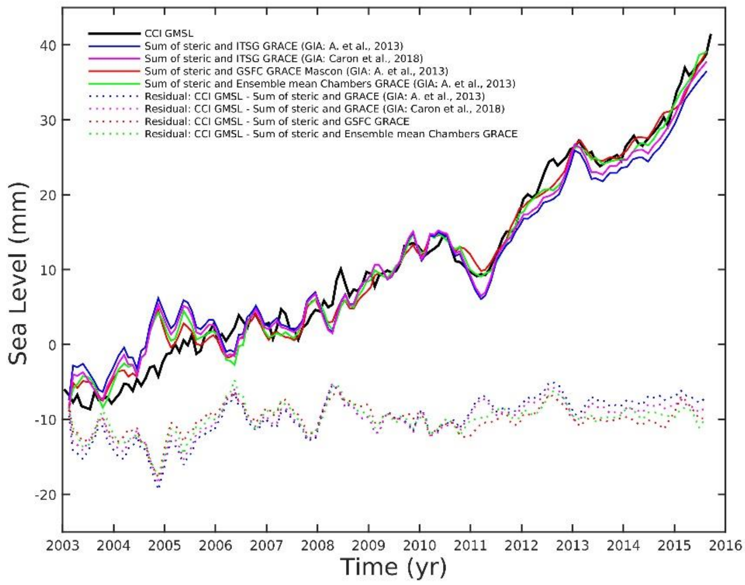

Figure 3.14: Observed CCI GMSL (black) superimposed with the GMSL estimated from the sum of steric v1.2 and various GRACE ocean mass products (colored solid lines) over 2003-2015. Their corresponding residual, i.e. $GMSL_{observed}$-$GMSL_{(steric+GRACE)}$ are also displayed as dotted lines.

3.2.3 Sea level budget for the ARGO/GRACE era 2005-2015 using CMEMS thermosteric data

We also performed the sea level budget analysis over 2005-2015 using the sum of v1 components and thermosteric sea level (0-2000 m) from CMEMS data.

Figure 3.15 displays the GMSL budget estimated as the sum of individual SLBC_cci v1 sea level components superimposed to the CCI observed altimetry based global mean sea level time series over 2005-2015 and its corresponding residual. The individual components are also displayed in the same figure. Table 3.9 displays the corresponding trend values and residual trend values. We can observe that using CMEMS thermosteric sea level time series closes the sea level budget with a residual of -0.11 mm/yr .

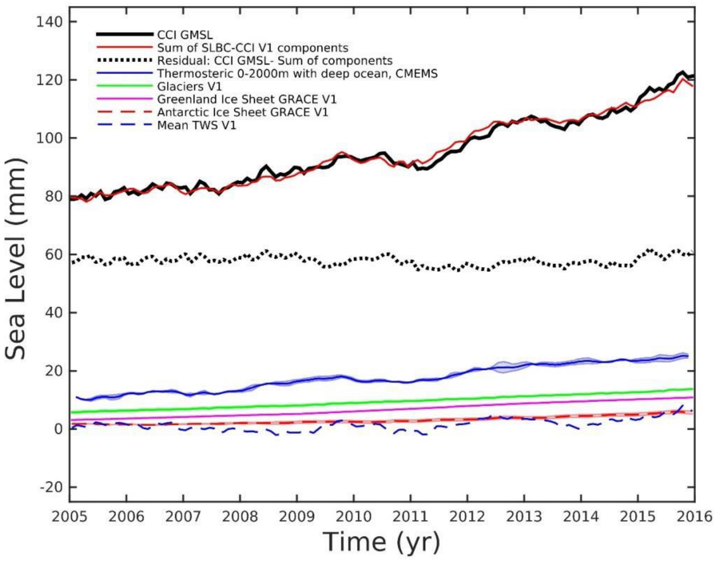

Figure 3.15: Observed CCI GMSL (black) superimposed with the GMSL estimated from the sum of SLBC_cci v1 sea level components (in red) over 2005-2015. The residual time series (i.e. CCI GMSL - sum of components) is shown as dotted black time series. The individual components, CMEMS thermosteric (in blue), glaciers (in green), Greenland (in magenta), Antarctica (dashed red) and TWS (dashed blue) are also displayed.

Table 3.9: Observed CCI GMSL trend compared with sum of components trend over 2005-2015.

Trend (mm/yr)	2005-2015
Observed CCI GMSL	**3.57 ± 0.3**
CMEMS thermosteric 0-2000 m	1.39
Antarctic Ice Sheet	0.39
Greenland Ice Sheet	0.75
Glacier	0.72
Total land Water Storage	0.43 ± 0.07
Sum of components	**3.68**
Residual	-0.11
RMS (mm)	7.0

3.3 Discussion and Conclusions

- Using v1 values for the components significantly improves closure of the sea level budget over both P(1) and P(2) periods. For 1993-2015, the residual trend and the RMS of the residuals amount to 0.18 mm/yr and 2.9 mm. For 2003-2015, the residual trend amounts to 0.2 mm/yr (or 0.17 mm/yr if GRACE AIS, GIS are used) and 0.31 mm/yr using the sum of mass components and GRACE ocean mass respectively. The RMS of the residual in the GRACE ocean mass case equals 2.96 mm (2.5 mm when using the GSFC GRACE mascon ocean mass).

- For some component data sets, the additional systematic trend uncertainty is not yet provided. This information will be needed for the final step of the project to complete the budget assessment with precise uncertainty range.

- The steric v1 time series has not been used because of computational problems (C. Merchant, personal communication) and has been replaced by v1.2 product over 2003-2015. The version 1.2 steric data proves to be better in terms of both interannual variability and trend over the period of study. Over 1993-2015 the steric ensemble mean time series used in Dieng et al. (2017) has been used since v1.2 does not cover the entire altimetry period. Furthermore, over 2005-2015, thermosteric data from Copernicus Marine Service (CMEMS) has also been used for comparison.

- Understanding discrepancies in TWS time series, as reported here between the WaterGap hydrological model and the two GRACE based TWS is very important. Closer investigations based on the GRACE TWS estimated at TU Dresden over land are needed for further understanding of these discrepancies.

- Variations of atmospheric water content were not considered here because uncertainties of available reanalysis products are not characterized for this purpose. Collaboration with the Water Vapour CCI and Clouds CCI project are addressed in the D1.3 "Roadmap towards a SLB_cci follow-on activity".

4 Arctic Sea Level Change

4.1 Data update

The DTU Arctic altimeter data base is presented in Figure 4.1. It is clear that distinct areas inside the Arctic Ocean only have availability less than 25%. As this is also seasonally dependent it can be concluded that large part of the Arctic Ocean offers limited altimeter-based estimates of sea surface height (ssh), in particular during winter. In turn, the time series and associated trends of altimeter-based ssh are inflicted with uncertainties.

The additional data used for the sea level budget assessment include:

- EN4, version 4 of the Met Office Hadley Centre "EN" series of global quality controlled ocean temperature and salinity profiles (T&S), only available to the end of 2013.
- Monthly gridded NERSC TOPAZ4 reanalyses data for the period 2003-2015.
- Mass changes from GRACE for the period 2003-2013 (GSFC RL5 mascons).

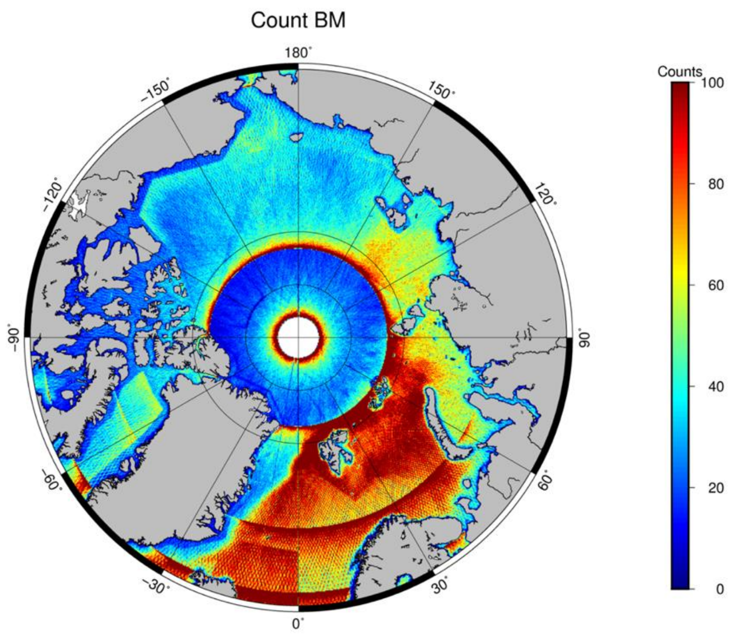

Figure 4.1: Illustration of the altimeter-based data coverage in % (color bar) for the Arctic Ocean and sub-Arctic seas.

.

4.2 Budget Assessment

In this version 1 of the assessment the coverage for the Arctic region is the entire ocean area north of 66°N. Note that the trends are only calculated for the time period up to 2013, primarily due to the fact that the EN4 data availability only exist to the end of 2013.

The TOPAZ sea level budget assessment is shown in Figure 4.2 (upper) while the observation-based budget assessment of the same quantities are shown in Figure 4.2 (lower). The latter reveal the presence of a residual of -1.1 mm/yr. The total ssh trend is clearly different with almost a doubling from the TOPAZ4 simulations (3.0 mm/yr) to the altimeter-based observations (5.7 mm/yr). The steric components, on the other hand, are comparable (1.2 mm/yr for TOPAZ4 versus 1.6 mm/yr for EN4). This is somewhat expected as TOPAZ4 is assimilating the EN4 data set. However, several distinct regional differences are noticed, such as in the Beaufort Gyre and the Lofoten basin within the Norwegian Sea. Finally, the trends in the mass change components are not comparable at all. Uncertainties in both components are to be considered. First, the TOPAZ4 value is simply emerging from the total ssh minus the steric component and is not properly accounting for the ice sheet melting and change of the

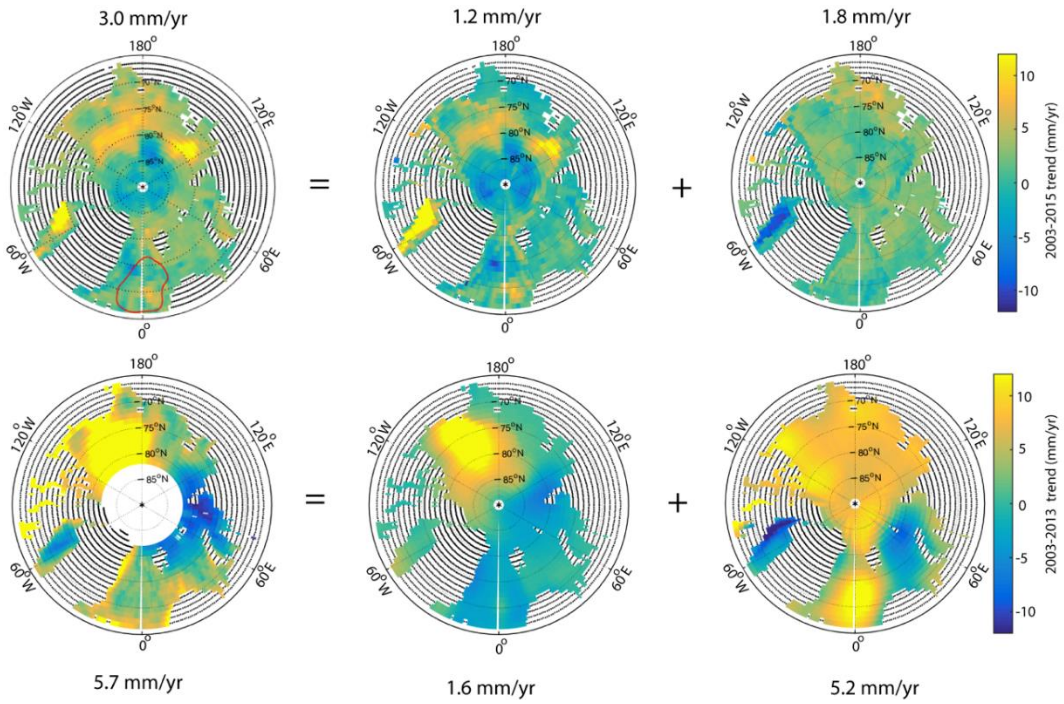

Figure 4.2: Budget assessment of the ssh (= steric + mass changes) for the Arctic region north of 66°N. Upper panel shows the result obtained from TOPAZ4 reanalysis for the period 2003-2015. Lower panel shows similar results based on observations from altimetry (ssh), steric (EN4) and mean mass changes (from three different GRACE model solutions) for the time period 1993-2013. The red polygon in the upper left panel indicates the Nordic Seas region used in Figure 4.4.

geoid. Second, the GRACE values are representing the mean from 3 different solutions, none of which have been adequately validated for the high latitude and Arctic Ocean. Moreover, there may be some leakage of mass changes over land that are wrongly invoked into the ocean signal due to the relative coarse spatial resolution of the GRACE data.

4.3 Discussion and Conclusions

In order to further assess these preliminary results the time series and corresponding mean linear trend estimates are compared in Figure 4.3 and Figure 4.4. This comparison includes the sea surface height (ssh) from altimetry, the mass changes derived from GRACE and ocean steric contribution derived from the EN4 in-situ climatology of temperature and salinity. The area coverage corresponds to the entire Arctic region outside the polar gap (Figure 4.3) and the Nordic Seas (Figure 4.4).

In addition, the contributions from the mass changes and steric components reveal strong differences, both for the entire Arctic region and the Nordic Seas. For the entire Arctic region the trend in the mass changes is more than 3 times as large as for the trend in the steric components. For the Nordic Seas only, the trends have, on the other hand, opposite signs, whereby the mass changes trend reaches more than 10 mm/yr in contrast to the trend of the steric component which is -2.5 mm/yr. In both cases it is noticed that the observed trends in ssh (5.7 mm/yr and 3.6 mm/yr) are dominated by the trends in the mass changes components (5.2 mm/yr and 10.2 mm/yr).

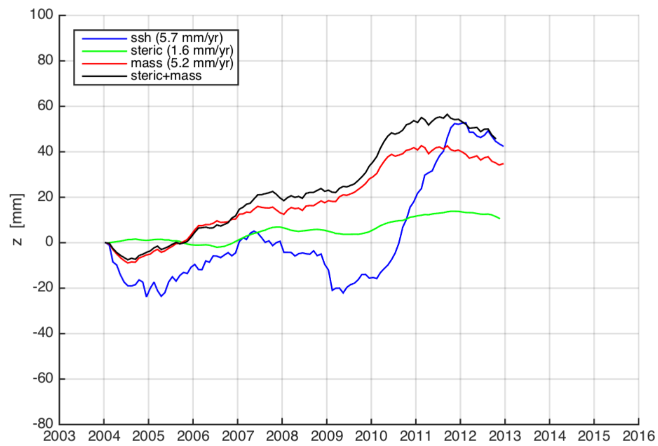

Figure 4.3: Time series (2 year running mean) and corresponding mean linear trend estimates of the sea surface height (ssh) from altimetry (blue), mass changes converted to ssh from GRACE (red), ocean steric contribution (green) and the sum of steric and mass (black) for the time period 2004 to 2013. Area corresponds to the entire Arctic region outside the polar gap.

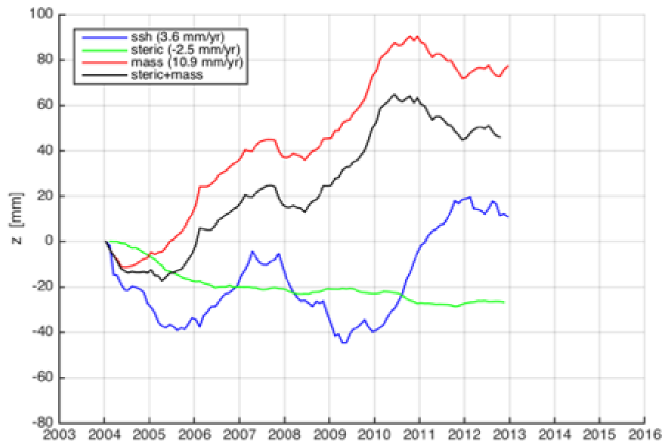

Figure 4.4: Same as Figure 4.3, but for the Nordic Seas (Area shown in Figure 4.2)

All in all these preliminary results suggest that:

(1) It is highly necessary to:

- Improve the geographical and seasonal altimeter coverage and reduce polar gap;
- Improve estimation of the steric component through more in-situ observations with better coverage;
- Create long time series from multiple altimeter satellites whereby biases connected with different corrections and processing methods are reliably removed;
- Perform a consistent correction for the inverse barometer effect (IBE).

(2) Closing of the regional sea level budget for the Arctic Ocean and neighboring seas at (seasonal) and annual time scale will depend on reliable estimates with uncertainties of the individual components, notably:

- proper estimates of seasonal bias in data coverage, especially wrt. sea ice;
- better estimate of leakage of signals in the GRACE data due to coarse spatial resolutions;
- including trend assessment for sub-regions, in addition to the entire region north of 66°N.

5 References

A, G., Wahr, J., and Zhong, S. (2013): Computations of the viscoelastic response of a 3-D compressible Earth to surface loading: an application to Glacial Isostatic Adjustment in Antarctica and Canada. *Geophysical Journal International*, 192(2), 557-572. doi: 10.1093/gji/ggs030.

Ablain M., R. Jugier, L. Zawadki, and N. Taburet (2017): *The TOPEX-A Drift and Impacts on GMSL Time Series*. AVISO Website. October 2017. https://meetings.aviso.altimetry.fr/fileadmin/user_upload/tx_ausyclsseminar/files/Poster_OSTST17_GMSL_Drift_TOPEX-A.pdf.

Bamber, J. L., Westaway, R. M., Marzeion, B., and Wouters,B. (2018):The land ice contribution to sea level during the satellite era, *Environ. Res. Lett.*, 13, 063008, doi: 10.1088/1748-9326/aac2f0.

Barletta, V. R., Sørensen, L. S., and Forsberg, R. (2013): Scatter of mass changes estimates at basin scale for Greenland and Antarctica. *The Cryosphere*, 7(5), 1411–1432

Caron, L., Ivins, E. R., Larour, E., Adhikari, S., Nilsson, J., and Blewitt, G. (2018): GIA model statistics for GRACE hydrology, cryosphere, and ocean science. *Geophysical Research Letters*, 45, 2203–2212. doi: 10.1002/2017GL076644.

Chambers, D. P., and J. A. Bonin (2012): Evaluation of Release-05 GRACE time-variable gravity coefficients over the ocean, *Ocean Sci.*, 8, 859–868, doi: 10.5194/os-8–859-2012.

Chen J. L., Wilson C. R., and Tapley B. D. (2013): Contribution of ice sheet and mountain glacier melt to recent sea level rise. *Nature Geoscience*, 6(7), 549-552.

Cogley, J.: Geodetic and direct mass-balance measurements: comparison and joint analysis, *Ann. Glaciol.,* 50, 96–100, 2009.

Dieng, H.B, A. Cazenave, B. Meyssignac, and M. Ablain (2017): New estimate of the current rate of sea level rise from a sea level budget approach, *Geophysical Research Letters*, 44, doi:10.1002/2017GL073308.

Gardner, A. S., Moholdt, G., Cogley, J. G., Wouters, B., Arendt, A. A., Wahr, J., Berthier, E., Hock, R., Pfeffer, W. T., Kaser, G., Ligtenberg, S. R. M., Bolch, T., Sharp, M. J., Hagen, J. O., van den Broeke, M. R., and Paul F. (2013): A reconciled estimate of glacier contributions to sea level rise: 2003 to 2009. *Science*, 340, 852– 857, doi: 10.1126/science.1234532.

Good, S. A., M. J. Martin, and N. A. Rayner (2013): EN4: Quality controlled ocean temperature and salinity profiles and monthly objective analyses with uncertainty estimates, *J. Geophys. Res. Oceans*, 118, 6704–6716, doi:10.1002/2013JC009067.

Horwath, M., and Groh, A. (2016): The GRACE mass change estimators developed for ESA's CCI ice sheet mass balance products. *Proc. GRACE Science Team Meeting 2016*, Potsdam, 5-7 November 2016. http://www.gfz-potsdam.de/en/section/global-geomonitoring-and-gravity-field/topics/development-operation-and-analysis-of-gravity-field-satellite-missions/grace/gstm/gstm-2016/proceedings/.

Ishii, M., and M. Kimoto (2009): Reevaluation of historical ocean heat content variations with time-varying XBT and MBT depth bias corrections, *J. Oceanogr.*, *65*(3), 287–299, doi:10.1007/s10872-009-0027-7.

Johnson, G. C., and D. P. Chambers (2013): Ocean bottom pressure seasonal cycles and decadal trends from GRACE Release-05: Ocean circulation implications. *J. Geophys. Res. Oceans*, 118, 4228–4240, doi: 10.1002/jgrc.20307.

Klinger, B., Mayer-Gürr, T., Behzadpour, S., Ellmer, M., Kvas, A., and Zehentner, N. (2016): The new ITSG-Grace2016 release. *Geophys. Res. Abstr.*, 18, EGU2016–11547.

Leclercq, P., Oerlemans, J., and Cogley, J. (2011): Estimating the glacier contribution to sea-level rise for the period 1800–2005, *Surv. Geophys.*, 32, 519–535.

Levitus S., et al. (2012): World ocean heat content and thermosteric sea level change (0–2000 m), 1955–2010. *Geophys. Res. Lett.*, 39, L10603. doi: 10.1029/2012GL051106.

Luthcke, S. B., Sabaka, T. J., Loomis, B. D., Arendt, A. A., McCarthy, J. J., and Camp, J. (2013): Antarctica, Greenland and Gulf of Alaska land-ice evolution from an iterated GRACE global mascon solution. *J. Glac.*, 59(216), 613–631. doi: 10.3189/2013JoG12J147.

Marzeion, B., Champollion, N., Haeberli, W., Langley, K., Leclercq, P., and Paul, F. (2017): Observation-Based Estimates of Global Glacier Mass Change and Its Contribution to Sea-Level Change, *Surv. Geophys.*, 28, 105–130, 2017.

Marzeion, B., Jarosch, A. H., and Hofer, M. (2012): Past and future sealevel change from the surface mass balance of glaciers, *The Cryosphere*, 6, 1295–1322, doi: 10.5194/tc-6-1295-2012.

Mayer-Gürr, T., Behzadpour, S., Ellmer, M., Kvas, A., Klinger, B., and Zehentner, N. (2016): ITSG-Grace2016 - Monthly and Daily Gravity Field Solutions from GRACE. *GFZ Data Services*. doi: 10.5880/icgem.2016.007.

Nagler, T., et al. (2016): *Comprehensive Error Characterisation Report (CECR)*. Antarctic_Ice_Sheet_cci project, ESA's Climate Change Initiative, version 1.1, 01 May 2016, Available from: http://www.esa-icesheets-antarctica-cci.org/.

Novotny, K., Horwath, M., et al. (2018*): ESA Climate Change Initiative (CCI) Sea Level Budget Closure (SLBC_cci)*. Product Description Document D2.3.2: Version 1 data sets and uncertainty assessments. Version 1.1.

Peltier W.R. (2004): Global glacial isostasy and the surface of the ice-age Earth: the ICE-5G (VM2) model and GRACE, *Annual Review of Earth and Planetary Sciences* 32:111.

Rignot, E. J., Velicogna, I., van den Broeke, M. R., Monaghan, A. J., and Lenaerts, J. T. M. (2011): Acceleration of the contribution of the Greenland and Antarctic ice sheets to sea level rise, Geophys. Res. Lett., 38, L05503, doi: 10.1029/2011GL046583.

Schröder, L., Horwath, M., Dietrich, R., Helm, V., Broeke, M. R., & Ligtenberg, S. R. (2019). Four decades of Antarctic surface elevation changes from multi-mission satellite altimetry. The Cryosphere, 13(2), 427-449.

Shepherd, A., Ivins, E. R., A, Geruo, Barletta, V. R., Bentley, M. J., Bettadpur, S., Briggs, K. H., Bromwich, D. H., Forsberg, R., Galin, N., Horwath, M., Jacobs, S., Joughin, I., King, M. A., Lenaerts, J. T. M., Li, J., Ligtenberg, S. R. M., Luckman, A., Luthcke, S. B., McMillan, M., Meister, R., Milne, G., Mouginot, J., Muir, A., Nicolas, J. P., Paden, J., Payne, A. J., Pritchard, H., Rignot, E., Rott, H., Sandberg Sorensen, L., Scambos, T. A., Scheuchl, B., Schrama, E. J. O., Smith, B., Sundal, A. V., van Angelen, J. H., van de Berg, W. J., van den Broeke, M. R., Vaughan, D. G., Velicogna, I., Wahr, J., Whitehouse, P. L., Wingham, D. J., Yi, D., Young, D., Zwally, H. J. (2012): A Reconciled Estimate of Ice-Sheet Mass Balance. *Science*, 338(6111):1183-1189, doi: 10.1126/science.1228102.

Shepherd, A., Ivins, E., Rignot, E., Smith, B., van den Broeke, M., Velicogna, I., et al. (2018). Mass balance of the Antarctic Ice Sheet from 1992 to 2017. Nature, 556, pages219-222.

Uebbing, B., J. Kusche, R. Rietbroek, and F. W. Landerer (2018): Processing choices affect ocean mass estimates from GRACE. *Journal of Geophysical Research: Oceans*, in review [as of 2018-09-28].

van den Broeke, M. R., E. M. Enderlin, I. M. Howat, P. Kuipers Munneke, B. P. Y. Noël, W. J. van de Berg, E. van Meijgaard and B. Wouters, 2016: On the recent contribution of the Greenland ice sheet to sea level change, The Cryosphere 10, 1933-1946, doi:10.5194/tc-10-1933-2016.

von Schuckmann K, and Le Traon P-Y (2011): How well can we derive Global Ocean Indicators from Argo data? *Ocean Sci.,* 7:783-791, doi: 10.5194/os-7-783-2011.

WCRP Global Sea Level Budget Group (the) (2018): Global sea level budget, 1993-present, *Earth System Science Data*, 10, 1551-1590, doi: 10.5194/essd-10-1551-2018.

WGMS (2016): *Fluctuations of Glaciers Database*. World Glacier Monitoring Service, Zurich, Switzerland. doi: 10.5904/wgms-fog-2016-08.

Appendix

CMC- Continental Mass Change from GRACE

Starting with the version 1 budget assessment, we also analyse mass changes from GRACE measurements over continents (without Greenland and Antarctica). As GRACE only made integral measurements of hydrological and ice mass changes, we compare the sum of LWS and glaciers with the CMC GRACE data (cf. Figure A 1). We observe a generally good agreement between the components, with a standard deviation of the misclosure - before removal of linear or seasonal signals - in the same order (2.95 mm) as for the OMC. However, a systematic periodic residual becomes visible in the misclosure plot (Figure A 1, bottom). Without further analysis, this effect may be attributed to systematic under-/overestimation in one of the components or to a systematic phase shift in the data.

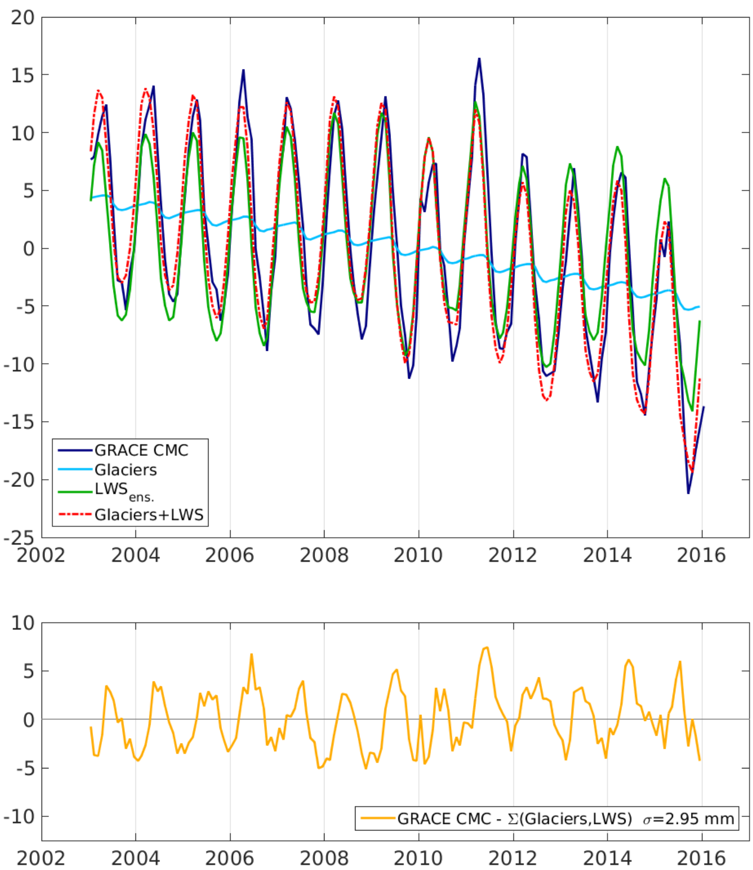

Figure A 1: Continental mass change from an ITSG-GRACE2016 based SLBC_cci version 1 solution (dark blue) and complementary sum (red) of glaciers (blue) and land water storage (green). The difference between GRACE solution and sum of glaciers and LWS has a STD of 2.95 mm for the series with the seasonal signals still included. This is the same range as for the v1 ocean mass budget (mis)closure. Further analyses of trends and removal of seasonal signals have yet to be accomplished.

End of document